Stratigraphy, provenance, and tectonic setting of the Lumsden Dam and Bluestone Quarry formations (Lower Ordovician), Halifax Group, Nova Scotia, Canada

Hayley D. Pothier[1,2], John W. F. Waldron[1]*, Chris E. White[3], S. Andrew Dufrane[1], and Rebecca A. Jamieson[4]

1. Department of Earth & Atmospheric Sciences, 1-26 Earth Science Building, University of Alberta, Edmonton, Alberta T6G2E3, Canada
2. Current address: Dassuault Systèmes GEOVIA Inc., 110 Yonge Street, Suite 1400, Toronto, Ontario M5C 1T4, Canada
3. Nova Scotia Department of Natural Resources, Halifax, Nova Scotia B3J 2T9, Canada
4. Department of Earth Sciences, Dalhousie University, Halifax, Nova Scotia B3H 4R2, Canada

*Corresponding author <john.waldron@ualberta.ca>

Date received: 04 October 2014 ¶ Date accepted: 11 January 2015

ABSTRACT

Cambrian to Ordovician metamorphosed clastic sedimentary rocks of the Meguma terrane have no correlatives elsewhere in Atlantic Canada but are similar to successions in North Wales. In the Meguma terrane, the Cambrian Goldenville Group, dominated by sandstone, is overlain by the Halifax Group, consisting mainly of fine-grained slate and siltstone. Within the Halifax Group widespread Furongian black slate units are overlain by greyer units with rare Early Ordovician fossils, assigned to the laterally equivalent Bear River, Feltzen, Bluestone Quarry, Lumsden Dam and Glen Brook formations. The type section of the Bluestone Quarry Formation, here defined, is on Halifax Peninsula, where four constituent members are recognized; the type section of the Lumsden Dam Formation is here defined in the Lumsden Dam region near Wolfville. Detrital zircons extracted from a sample of the Lumsden Dam Formation show a range of ages similar to those displayed by the underlying Goldenville Group, including abundant Neoproterozoic zircon representing Avalonian or Pan-African sources, and a prominent group of peaks between 1.95 and 2.2 Ga, probably representing sources in West Africa. A sample from the Glen Brook Formation east of Halifax shows a similar distribution. In contrast to the correlative Welsh successions, no influx of Mesoproterozoic zircon is seen in Early Ordovician samples, suggesting that, if the two basins were in close proximity in the Cambrian, they had diverged by the Early Ordovician, possibly as a result of strike-slip motion along the margin of Gondwana.

RÉSUMÉ

Les roches sédimentaires clastiques métamorphisées du Cambrien à l'Ordovicien du terrane de Meguma n'ont pas de corrélatif ailleurs au Canada atlantique, mais sont semblables à des successions observées en Galles du Nord. Dans le terrane de Meguma, le groupe de Goldenville du Cambrien, à prédominance de grès, est recouvert du groupe d'Halifax, pour sa part composé principalement de siltite et d'ardoise à grains fins. Au sein du groupe d'Halifax, d'importantes unités d'ardoise noire du Furongien sont recouvertes d'unités plutôt grises et de rares fossiles de l'Ordovicien précoce attribués aux formations latéralement équivalentes de Bear River, de Feltzen, de Bluestone Quarry, de Lumsden Dam et de Glen Brook. Le stratotype de la formation de Bluestone Quarry est ici défini comme se trouvant sur la péninsule d'Halifax, où on reconnaît quatre membres constitutifs, tandis que le stratotype de la formation de Lumsden Dam est ici défini comme se trouvant dans la région de Lumsden Dam, près de Wolfville. Des zircons détritiques extraits d'un échantillon de la formation de Lumsden Dam révèlent différents âges semblables à ceux du groupe de Goldenville sous-jacent. On y trouve notamment une abondance de zircon du Néoprotérozoïque représentant des sources avaloniennes ou pan-africaines et un groupe proéminent de pics âgés de 1,95 à 2,2 Ga représentant probablement des sources de l'Afrique de l'Ouest. Un échantillon de la formation de Glen Brook, située à l'est d'Halifax, révèle une distribution semblable. À la différence des successions du Pays de Galles qui y sont liées, aucun afflux de zircon du Mésoprotérozoïque n'est observé dans les échantillons de l'Ordovicien précoce, ce qui tend à indiquer que les deux bassins, qui étaient situés tout près au Cambrien, se sont éloignés à l'Ordovicien précoce, vraisemblablement à la suite d'un mouvement de décrochement le long de la limite de Gondwana.

[Traduit par la redaction]

0843-5561|15|00051-083 $5.95|0

INTRODUCTION

Metamorphosed clastic sedimentary rocks of the Meguma terrane (Fig. 1), the most outboard terrane of the Canadian Appalachians, have no correlatives elsewhere in Atlantic Canada, and their source has been the subject of disagreement. The terrane resided along the northern margin of Gondwana during the Cambrian; however, its exact position along this margin relative to West Africa and Amazonia, and to other peri-Gondwanan terranes, remains uncertain (e.g., Schenk 1997; Waldron *et al.* 2009).

The Meguma terrane takes its name from a distinctive stratigraphic unit, named the Meguma Series by Woodman (1904) and subsequently termed the Meguma Group (Stevenson 1959) or Supergroup (Schenk 1995a, 1997). It comprises the Cambrian to Early Ordovician Goldenville and Halifax groups (Schenk 1995a; White 2010a), which are overlain by the Silurian to Devonian Rockville Notch Group (White 2010a, White *et al.* 2012), all of which are intruded by mainly Late Devonian plutons (Clarke and Halliday 1980). Recent mapping of the Meguma terrane in Nova Scotia has led to the identification and division of several mappable units within the Halifax and Goldenville groups (White 2010b). In this paper we formally define the Lumsden Dam and Bluestone Quarry formations of the upper Halifax Group in the Wolfville and Halifax regions. Although type sections for the remaining units have yet to be defined, they have been named as formations, and to avoid confusion we here follow the suggestion of a reviewer and the journal editors and use formal nomenclature (e.g., Cunard Formation) for all of these units pending future formal definition of type sections. Both the Lumsden Dam and Bluestone Quarry formations record similar sedimentological features, and the presence of a mass transport deposit in the Bluestone Quarry Formation suggests they were deposited in a slope environment. Here we also pres-

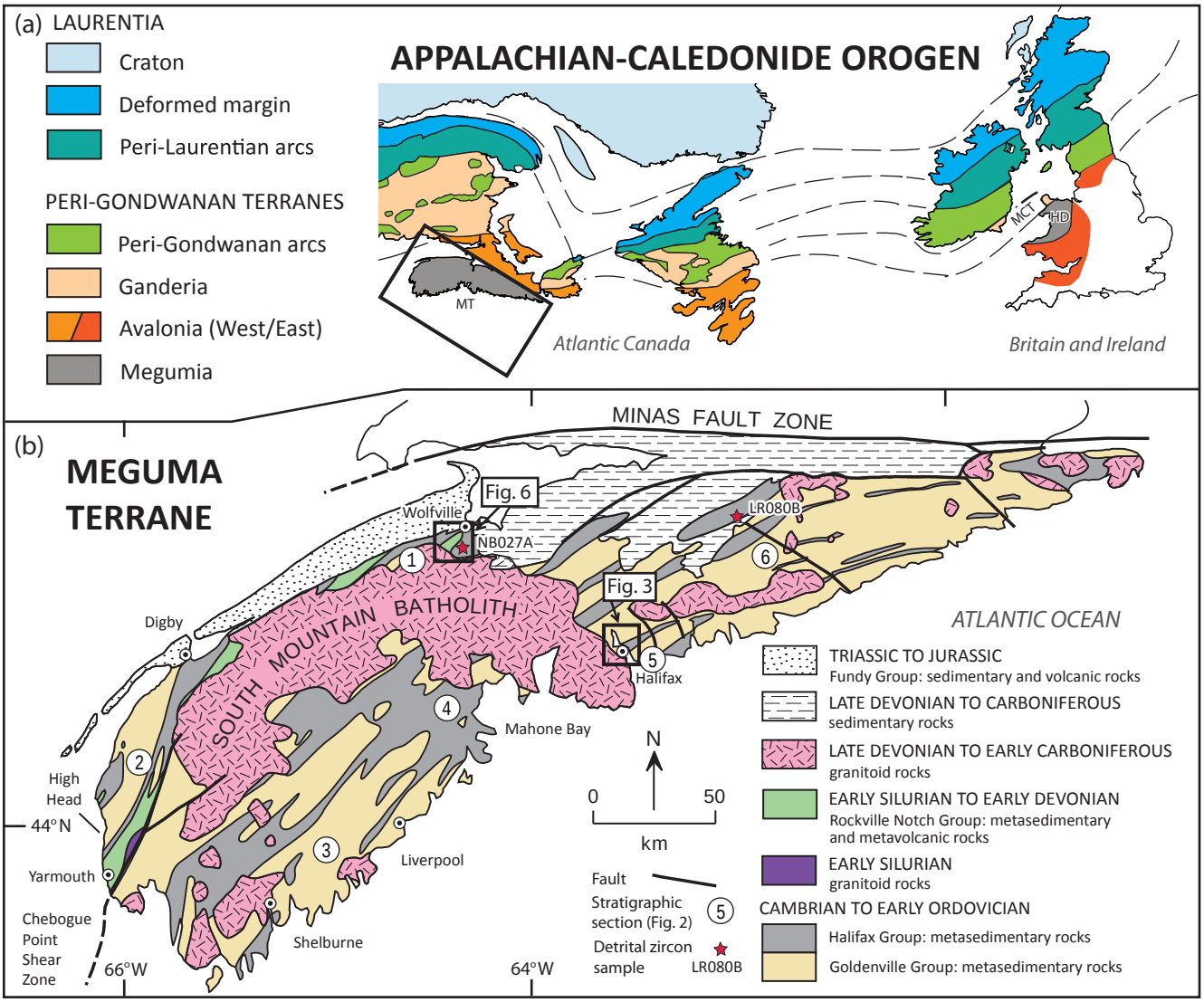

Figure 1. Meguma terrane (after White 2010b) with inset map showing its location in the northern Appalachian-Caledonide orogen (after Hibbard *et al.* 2006). Boxes show location of maps shown in Figs. 3 and 6. Numbers refer to stratigraphic columns shown in Fig. 2. Abbreviations: HD - Harlech Dome; MCT - Monian composite terrane; MT - Meguma terrane.

ent the first detrital zircon data from the Halifax Group, which complement previous provenance studies conducted in the Goldenville and Rockville Notch groups (Krogh and Keppie 1990; Murphy *et al.* 2004b; Waldron *et al.* 2009) and in correlative units in the British Isles (Pothier *et al.* 2014). The data show similar distributions to underlying units, and are consistent with a primary West African source region with a minor input of Amazonian detritus.

GEOLOGIC SETTING

Meguma terrane

The Meguma terrane is exposed south of the Minas Fault Zone in Nova Scotia (Fig. 1). The thick (>13 km) Cambrian-Ordovician variably metamorphosed sandstone-shale succession of the Goldenville and Halifax groups is overlain unconformably by Silurian-Devonian volcanic-sedimentary rocks of the Rockville Notch Group (White *et al.* 2012). This succession has been deformed into SW-NE trending folds during the Middle Devonian Neoacadian orogeny (van Staal 2007; White *et al.* 2007), and were intruded by the South Mountain Batholith and other plutons during the Late Devonian (Clarke and Halliday 1980). Regional metamorphism is greenschist facies (chlorite-biotite zones) with low-pressure amphibolite facies (andalusite-staurolite-cordierite zones) in southwestern and eastern mainland Nova Scotia (Keppie and Muecke 1979; Raeside and Jamieson 1992). Low-pressure (andalusite-cordierite-K-feldspar zones) contact metamorphism is present within ca. 2 km of the contact with the South Mountain Batholith and numerous smaller plutons (Jamieson *et al.* 2012). Unconformably overlying the Meguma terrane and adjacent Avalonia are the Late Devonian to Carboniferous successions of the Maritimes Basin and the Mid-Triassic to Early Jurassic Fundy Group (Klein 1962; Martel and McGregor 1993).

The Chebogue Point Shear Zone (CPSZ) is located in southwestern Nova Scotia in the Yarmouth region (Fig. 1). It strikes N-S to NE-SW (White 2010b) and is assumed to pass into the South Mountain Batholith, although has not been clearly traced east of its intersection with the batholith. White (2010b) has described the CPSZ as a tectonostratigraphic boundary, dividing the Meguma Supergroup into different, though correlative, units at the formation level, lying to the northwest and southeast of the shear zone and South Mountain Batholith.

Basement characteristics such as age, deformation, and composition normally provide critical information about a terrane's origin; however, Meguma terrane basement rocks are not exposed anywhere in Nova Scotia. Sm-Nd isotopic studies on Meguma granitoid rocks (Clarke *et al.* 1988) and basement xenoliths (Eberz *et al.* 1991) indicate that the deeper crust includes material with a younger residence age than the overlying Meguma Supergroup. Greenough *et al.* (1999) dated zircon and monazite from basement xenoliths, which showed a Pan-African – Avalonian population (575–630 Ma), with a possible Mesoproterozoic grain population defined by the upper intercepts of a discordant zircon fraction. These data were interpreted by Greenough *et al.* (1999) to suggest that the Meguma succession rests upon a basement with Avalonian affinities. It has been proposed that the West Avalonia and the Meguma terrane once formed a part of the same microcontinent and that the Meguma succession was deposited on Avalonian crust (e.g., Keppie *et al.* 1997; Landing 2004; Murphy *et al.* 2004a; Linnemann *et al.* 2012). Others interpret the contact between the two terranes as a thrust (e.g., Eberz *et al.* 1991; Keppie and Dallmeyer 1987; Waldron *et al.* 1989; Greenough *et al.* 1999) along which the Meguma terrane was emplaced over Avalonia.

Goldenville Group

The Goldenville Group (Fig. 2) is the oldest unit in the Meguma terrane, and spans the early Cambrian (Terreneuvian) to the early Furongian (White *et al.* 2012). It is primarily composed of thick-bedded metamorphosed sand-rich turbidites with local interbedded siltstone and slate (Harris and Schenk 1976; Waldron and Jensen 1985) with an estimated thickness of ≥8000 m (White *et al.* 2012). The highest part of the Goldenville Group is characterized by manganese-rich slate and siltstone (e.g., Waldron 1992). In southwestern Nova Scotia, the High Head member (Fig. 2) contains abundant trace fossils, including *Oldhamia*, that are characteristic of the early Cambrian (Gingras et al. 2011). These fossils are consistent with detrital zircon collected from the Church Point Formation (Fig. 2) that suggested a maximum depositional age close to the Ediacaran-Terreneuvian boundary (Waldron *et al.* 2009). In southern Nova Scotia, the Government Point Formation (Fig. 2) yielded a middle Cambrian (Epoch 3) Acado-Baltic trilobite faunule (Pratt and Waldron 1991).

Halifax Group

The Halifax Group spans the Furongian to Lower Ordovician (Fig. 2) and is generally much finer grained than the underlying Goldenville Group (White *et al.* 2012). The lowest unit in the Halifax Group as defined by White (2010b) is the Cunard Formation in the Halifax region and its correlatives, the Acacia Brook and North Alton formations in the Digby-Yarmouth and Wolfville regions (Fig. 2, 3a). These units are strongly cleaved, dark grey to black slate, with thin lenses and beds of metamorphosed siltstone and fine- to medium-grained sandstone. They contain abundant sulphide minerals (dominantly pyrrhotite) and weather rusty brown. An acritarch assemblage sampled from the North Alton Formation indicates a Jiangshanian (mid-Furongian) age (White *et al.* 2012). Conformably above these units are the regionally correlative Lumsden Dam, Bluestone Quar-

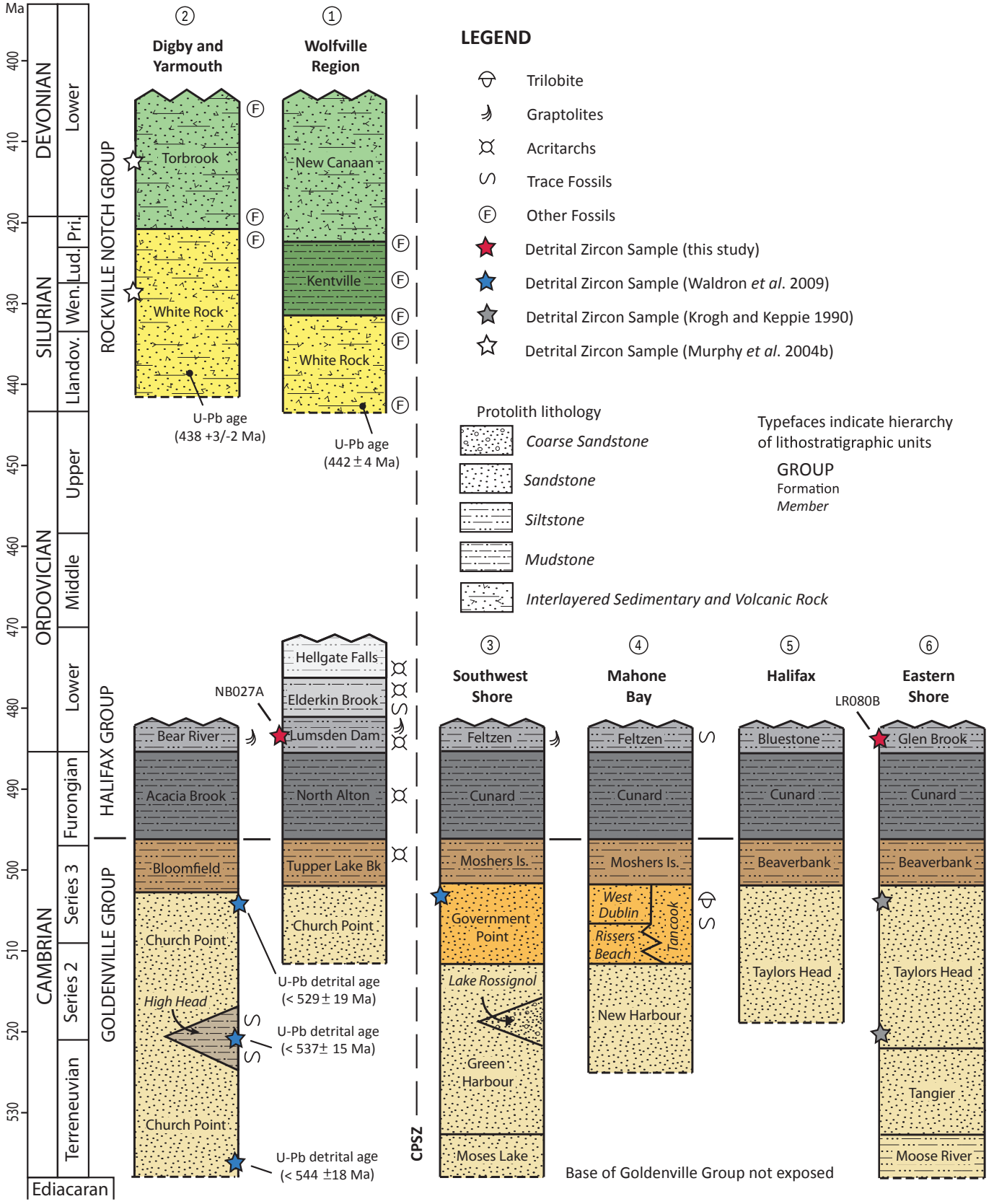

Figure 2. Generalized stratigraphy of the Meguma terrane in different regions in Nova Scotia (after O'Brien 1988; Horne and Pelly 2007; White 2010b; White *et al.* 2012) showing the locations sampled in detrital zircon studies. Paleontological and U-Pb age data are from sources described in the text. Time scale of Peng *et al.* (2012).

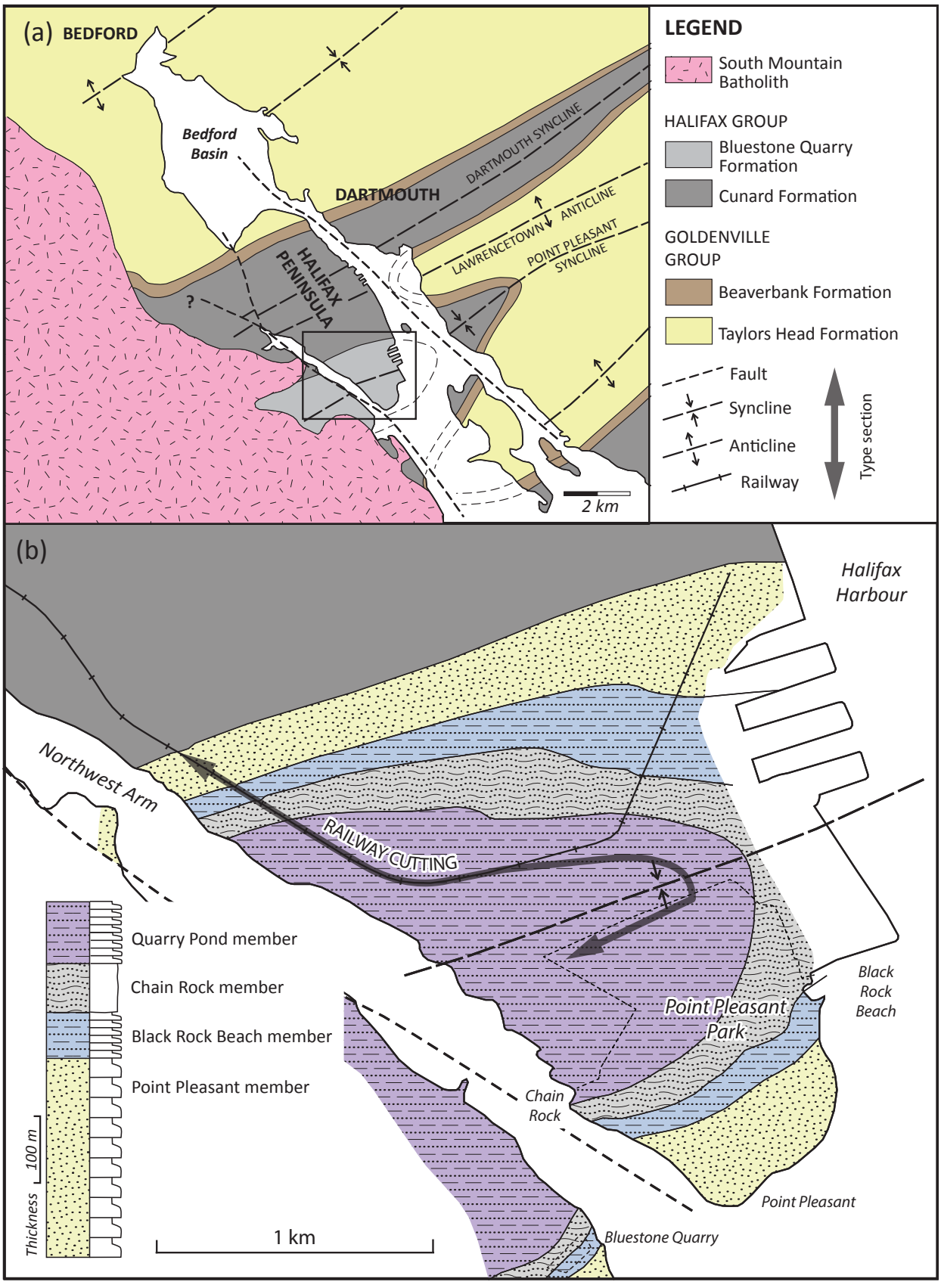

Figure 3. Geological map of (a) the Halifax area after White *et al.* (2008) and (b) the Bluestone Quarry Formation (after Jamieson *et al.* 2011).

ry, Glen Brook, Feltzen, and Bear River formations (Fig. 2). These formations, which are the focus of the remainder of the paper, comprise light to dark grey slate interlayered with cross-laminated siltstone and fine-grained sandstone. They contain noticeably less pyrrhotite, pyrite, and arsenopyrite than the underlying formations. Tremadocian graptolite fossils are preserved in the Bear River, Feltzen, and Lumsden Dam formations (White 2010a).

The uppermost units of the Halifax Group are preserved only in the Wolfville area. The Elderkin Brook Formation (Fig. 2) conformably overlies the Lumsden Dam Formation. It consists of diffusely to finely laminated, cleaved mudstone. Unlike the Lumsden Dam Formation this unit lacks cross-laminated siltstone and sandstone beds, but is mildly bioturbated. Its colour ranges from pale greenish grey to medium grey, and it weathers to a purple-red colour in places. Acritarch and trace fossils in this unit indicate late Tremadocian age (White *et al.* 2012). The overlying Hellgate Falls Formation (Fig. 2; White 2010a), is light to dark grey slate interbedded with light to dark grey thin siltstone and sandstone beds and lenses. Abundant bioturbation textures and trace fossils characterize this unit. Locally, black slate occurs at the very top of the formation (White 2010a). It is disconformably overlain by the Silurian White Rock Formation (White 2010a). The age of the Hellgate Falls Formation is constrained by Early Ordovician acritarch fossils, which range from the latest Tremadocian to Floian (White *et al.* 2012).

Rockville Notch Group

The Silurian to Lower Devonian Rockville Notch Group (formerly the Annapolis Supergroup of Schenk 1995b) is preserved on the northwest side of the CPSZ and South Mountain Batholith (Fig. 2). The basal White Rock Formation, which rests unconformably over the Halifax Group (White 2010a), comprises shallow marine metamorphosed sedimentary (Lane 1975; Bouyx *et al.* 1997) and rift-related volcanic rocks (Schenk 1997; Keppie and Krogh 1999; MacDonald *et al.* 2002). A rhyolite near its base produced an early Llandovery U-Pb zircon age of 442 ± 4 Ma (Keppie and Krogh 2000) and a felsic tuff higher in the formation in the Yarmouth area produced a mid-Llandovery age of 438 ± 3 Ma (MacDonald *et al.* 2002). The White Rock Formation is overlain by siltstone and slate of the Kentville Formation (Smitheringale 1960; Taylor 1965). The Kentville Formation contains graptolites and microfossils (Smitheringale 1973; Bouyx *et al.* 1997) indicative of a late Wenlock to early Pridoli (Silurian) age. The Kentville Formation is overlain by Pridoli to upper Lower Devonian (Smitheringale 1973; Bouyx et al. 1997) marine sedimentary and volcanic rocks of the New Canaan and Torbrook formations (Smitheringale 1960; Taylor 1965).

FORMAL DESCRIPTIONS

White (2010b) has provided a review of the informal stratigraphic subdivisions within the Goldenville and Halifax groups established during mapping in the Meguma terrane. Herein, we formally define two of the regionally correlative units in the upper part of the group, the Bluestone Quarry and Lumsden Dam formations and present more detailed descriptions of these formations to better define the environment of deposition and regional tectonic significance of the sedimentary rocks in the upper part of the Halifax Group. All coordinates are based on the Universal Transverse Mercator (UTM) projection, using North American Datum 1983.

Bluestone Quarry Formation

The Bluestone Quarry Formation is mappable in the Halifax area where it is exposed in the core of a SW-plunging syncline in Point Pleasant Park, in an adjacent railway cut, and in numerous other exposures on both sides of Northwest Arm (Fig. 3). It was recognized as a distinctive unit (Bluestone member of the Halifax Formation) by Jamieson *et al.* (2005), and named Bluestone Formation by White *et al.* (2008); the unit is here named Bluestone Quarry Formation to avoid confusion with a similarly named unit in West Virginia, USA (Cardwell *et al.* 1968). The name is derived from a quarry located immediately SW of Northwest Arm (Jamieson *et al.* 2012), the source of a common building stone in the Halifax area. The unit conformably overlies graphitic, sulphide-rich slate and hornfels of the Cunard Formation. The rocks of the Bluestone Quarry Formation are interbedded light grey to beige sandstone and siltstone with medium to dark grey slate, variably overprinted by contact metamorphism. Bedding is continuous at the outcrop scale (several metres). Beds are graded and have sharp, flat bases, with scour structures in places. Sandstone commonly appears massive to parallel or cross-laminated; siltstone is most often cross-laminated, and slate exhibits weak parallel to wavy laminae. The cross-laminae show unidirectional current flow, typically with a northward component, and the ripples have sinuous crest morphologies. Trough cross-laminations and climbing-ripple cross-laminations are common (Fig. 4).

The Bluestone Quarry Formation lacks the abundant sulphide minerals present in the underlying Cunard Formation. It contains carbonate concretions that have locally been metamorphosed to calc-silicate rock (Jamieson *et al.* 2005, 2012). The concretions, which are broadly parallel to, but overprint bedding, typically lie within the upper parts of siltstone and sandstone beds; this association helps to distinguish this unit from the underlying Cunard Formation. Much of the Bluestone Quarry Formation lies within the contact aureole of the South Mountain Batholith (Halifax Pluton), where the regional chlorite zone assemblage is

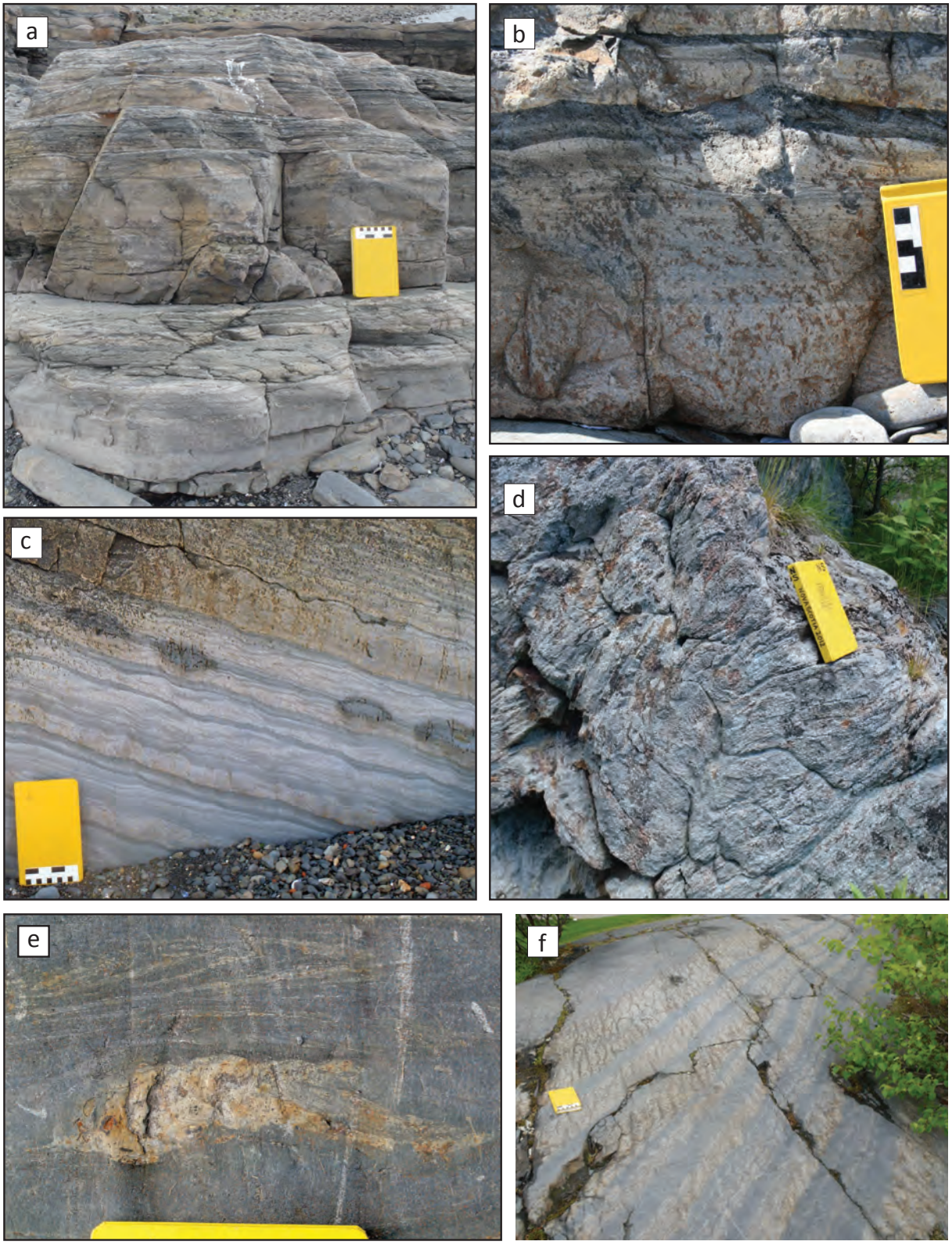

Figure 4. Typical field appearances of the Bluestone Quarry Formation: (a–b) Point Pleasant member, showing thick sandstone beds with well developed Bouma "B" divisions of parallel-laminated sandstone; (c) Black Rock Beach member showing abundant thinly bedded siltstone and sandstone beds with ripple cross-laminations; bed in middle of view shows four oval carbonate-bearing concretions; (d) Chain Rock member showing folded bedding; (e) Chain Rock member showing isolated sandstone lens; (f) Quarry Pond member showing thinly bedded graded siltstone; climbing ripple cross-lamination is distorted by tectonic deformation and emphasized by differentiated cleavage.

overprinted by the assemblage cordierite + biotite ± andalusite, and the slaty cleavage is annealed within ca. 1 km of the contact (Jamieson *et al.* 2012). Compositional differences from the adjacent Cunard Formation produce distinctive metamorphic mineral assemblages and isograds within the Bluestone Quarry Formation, which have proven useful in mapping the boundary (Jamieson *et al.* 2005; Jamieson *et al.* 2012).

The type section for the Bluestone Quarry Formation is located along the railway cutting and in adjacent Point Pleasant Park (Fig. 3), where the formation outcrops almost in its entirety. The Bluestone Quarry Formation is here divided into four informal members: the Point Pleasant member, the Black Rock Beach member, the Chain Rock member, and the Quarry Pond member (Fig. 3; following Jamieson *et al.* 2011). The basal contact of the formation (Fig. 5), exposed in the railway cutting [20T 453021E 4942263N], is conformable and is defined within a gradational transition at the lowest occurrence of fine-grained metamorphosed sandstone beds (Point Pleasant member) with carbonate concretions (Fig. 5). The highest part of the section (Quarry Pond member) in the type area occurs in the core of the Point Pleasant syncline. No overlying strata other than Quaternary deposits are observed in the Halifax region, where the Bluestone Quarry Formation is the youngest exposed bedrock unit; thus an upper stratigraphic contact cannot be defined. The minimum thickness of the Bluestone Quarry Formation is estimated to be 531 m. Additional descriptions are provided in a companion paper which focusses on the interpretation of the Chain Rock member (Waldron *et al.* 2015).

The lowest, Point Pleasant member (approximately 295 m thick) is well exposed inland and along the shoreline in the south end of Point Pleasant Park (Fig. 3). It comprises thinly to thickly bedded (bed-thickness terminology after Boggs 2001) high-energy turbidite deposits and is the most sand-rich member (Figs. 4a, b). Bouma divisions A through to E are common, but partial Bouma sequences are also present, where the basal divisions are missing or just divisions A and E are preserved. The interbedded slates are distinctly darker, and more graphitic than in the higher parts of the formation.

The Black Rock Beach member is ~68 m thick and is best exposed at Black Rock Beach (Fig. 3). The member contains very thin- to medium-bedded low energy turbidite deposits (Figs. 4c, 5). Bouma divisions C–E and D–E are common, but Bouma A divisions are absent.

The Chain Rock member is ~75 m thick and is more resistant to erosion than the other members, forming a high ridge within Point Pleasant Park (Fig. 3). It is characterized by bedding that is variably folded, discontinuous, or completely disordered, with isolated blocks of siltstone and sandstone within a featureless matrix (Fig. 4d, e), described in more detail in a companion paper (Waldron *et al.* 2015). The deformation and disruption of bedding pre-dated the development of the regional slaty cleavage, but post-dated the formation of the carbonate concretions (Jamieson *et al.* 2011). On the east coast of the Northwest Arm, and in the region of Bluestone Quarries to the west, the contact with the underlying Black Rock Beach member is visible [20T 445499E 4940918N]. The sharp contact appears to be an erosional surface where the Chain Rock member incises into the underlying unit. Due to the stratiform geometry and chaotic deformational style of the Chain Rock member it is interpreted as a downslope mass-transport deposit (Jamieson *et al.* 2011; Waldron *et al.* 2015).

The Quarry Pond member has a minimum thickness of 93 m. It is best exposed in the railway cutting (Fig. 3) and also forms scattered outcrops within Point Pleasant Park and in adjacent residential subdivisions. This member is very similar to the Black Rock Beach member as it also consists of very thin- to medium-bedded, low-energy turbidite deposits in which Bouma divisions C–E and D–E are common (Fig. 4f). The Quarry Pond member is the highest unit in the formation and occupies the core of the Point Pleasant syncline; its original top is not exposed, but it is unconformably overlain by unconsolidated Quaternary sediments.

The age of the Bluestone Quarry Formation is not well constrained, as no body fossils have been found in this area (White *et al.* 2008). A single occurrence of deformed burrows was reported by Hart (2006). Based on its stratigraphic position above the Cunard Formation, the Bluestone Quarry Formation has been correlated with the unfossiliferous Glen Brook Formation (Fig. 2), and with the Lumsden Dam, Feltzen, and Bear River formations, which contain graptolite and acritarch fossils of Tremadocian age (White *et al.* 2012). This provides the best estimate for the age of the Bluestone Quarry Formation, assuming the contacts are not diachronous.

Lumsden Dam Formation

The divisions of the Halifax Group in the Wolfville region, including the Lumsden Dam Formation, were first described and informally named by White (2010b). In the Wolfville region, the Lumsden Dam Formation is exposed on the northwest limb of an anticline (Fig. 6). Excellent exposure of the unit can be seen in the Black River area, the best exposures being in an overflow channel located to the northwest of Lumsden Dam. This section has roughly 200 m of continuous outcrop (Fig. 7). The continuous outcrop terminates southward at the south end of the channel cut [20T 389943E 986789N]; to the north it disappears under vegetative cover [20T 389878E 4986982N]. Sedimentary structures were difficult to observe along the cliff edge of the channel, but were easily seen on adjacent areas of flat exposure (Fig. 8, 9). The remainder of the type section is defined in intermittent exposure to the north and south of this well exposed section.

The Lumsden Dam Formation consists mainly of metamorphosed light grey siltstone and dark grey mudstone

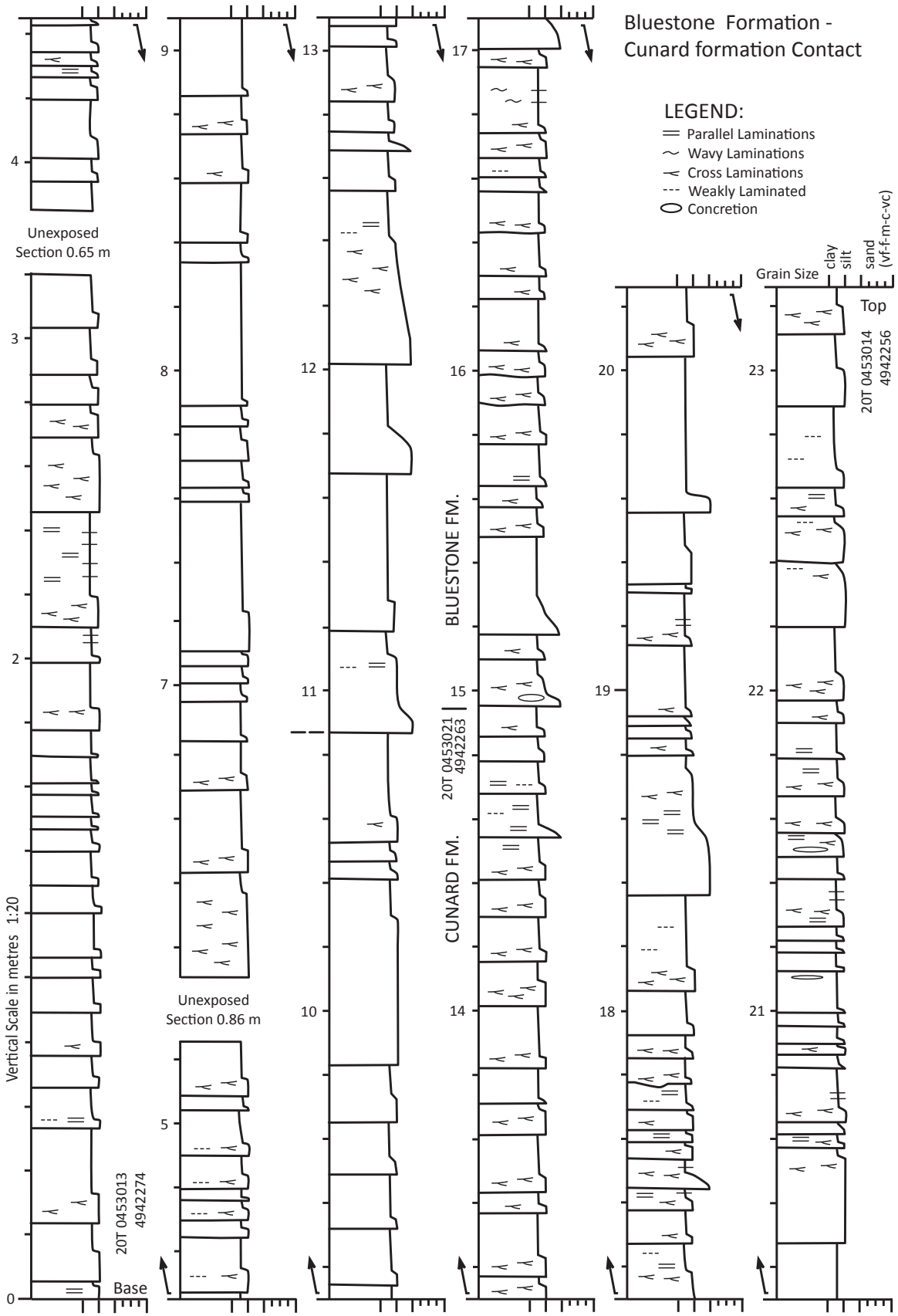

Figure 5. Detailed section of the contact between the Cunard and Bluestone Quarry formations.

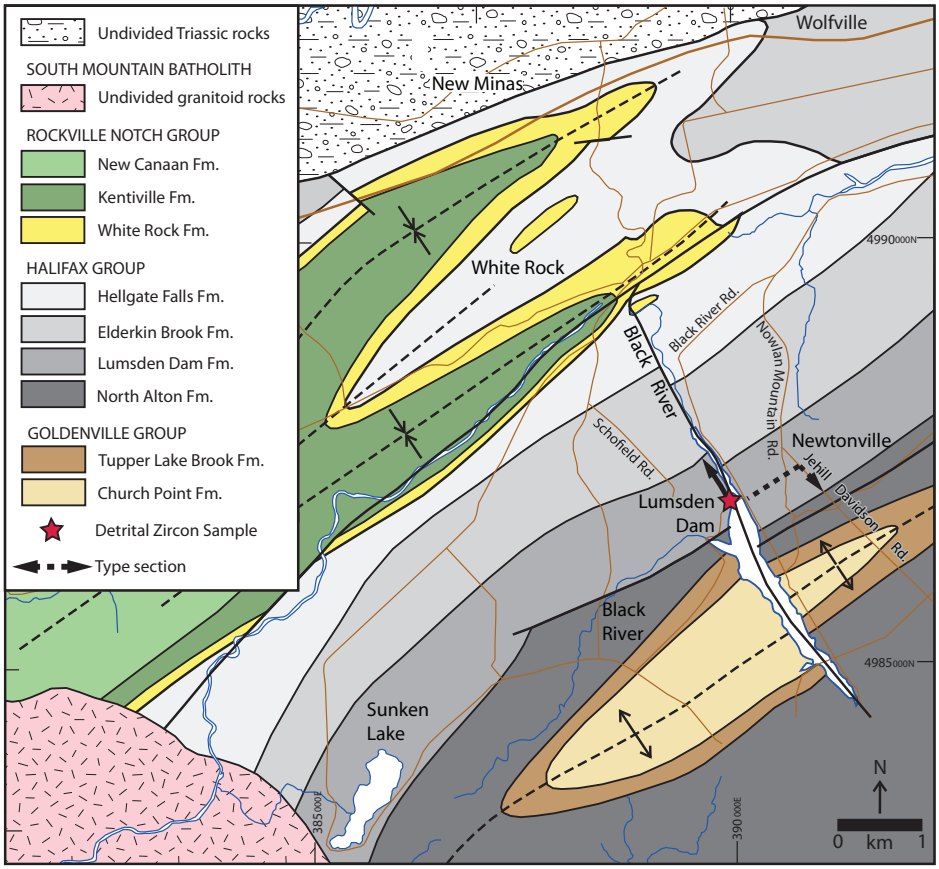

Figure 6. Geological map of the Wolfville area (after White 2010a).

with minor very fine-grained sandstone (Fig. 9). Graded beds are prevalent throughout the section and are very thin (1–3 cm) to medium (10–30 cm) bedded. Siltstone and sandstone beds are parallel laminated to cross-laminated, while most mudstone layers contain thin parallel laminae of silstone. Thicker siltstone and sandstone beds are laterally continuous at the outcrop scale (several metres), but thin (less than 2 cm) cross-laminated beds commonly appear as lenses or as semi-continuous and lenticular (Fig. 9c). Bed bases are sharp and flat with some scouring.

The Lumsden Dam Formation contains minor sulphide minerals (noticeably less than the underlying North Alton Formation) and it weathers to rusty brown. Rare, small (1–3 cm) carbonate concretions are also found within the siltstone and sandstone beds. The section contains four mafic intrusions that were emplaced parallel to bedding. These fine-grained, medium grey sills range in thickness from 90 to 120 cm and are easily confused with thick sandstone beds, as they are similar in field appearance to the coarser units of the host Lumsden Dam Formation (Figs. 7, 9d).

The boundary between the Lumsden Dam Formation and the underlying North Alton Formation is located along Jehill Davidson Road in Newtonville (Fig. 6). Intermittent exposure along the roadbed shows a change from dominantly medium grey to black mudstone with locally abundant sulphides and siltstone beds less than 10 cm thick in the North Alton Formation, up into dominantly medium grey to greenish-grey mudstone with siltstone and sandstone beds that reach thicknesses greater than 10 cm in the Lumsden Dam Formation. The boundary is placed at the lowest occurrence of a siltstone bed with thickness greater than 10 cm [20T 391089E 4986980N]. White *et al.* (2012) have described the contact as gradational over an interval of 5 m in continuous exposure revealed temporarily during the draining of Lumsden Lake, and in other parts of the region.

The boundary between the Lumsden Dam Formation and the overlying Elderkin Brook Formation is not visible along the east side of Black River Road, but is constrained within 62 m between coordinates 20T 389838E 4987401N and 20T 389815E 4987459N. Here there is a transition from the Lumsden Dam Formation, which contains siltstone and thick cross-laminated sandstone, into thick laminated mudstone with only minor siltstone of the Elderkin Brook Formation (Fig. 9e). The boundary is placed at the highest occurrence of a siltstone bed thicker than 2 cm. In the studied area the Lumsden Dam Formation is estimated to be 550 m thick, although White (2010a) suggested it could reach up to 1500 m thick in some areas.

The graptolite *Rhabdinopora flabelliformis flabelliformis* has been identified (White *et al.* 2012) in beds near the middle of the Lumsden Dam Formation (Fig. 9b), and acritarch assemblages restrict the age of the Lumsden Dam Formation to the early to middle Tremadocian (White *et*

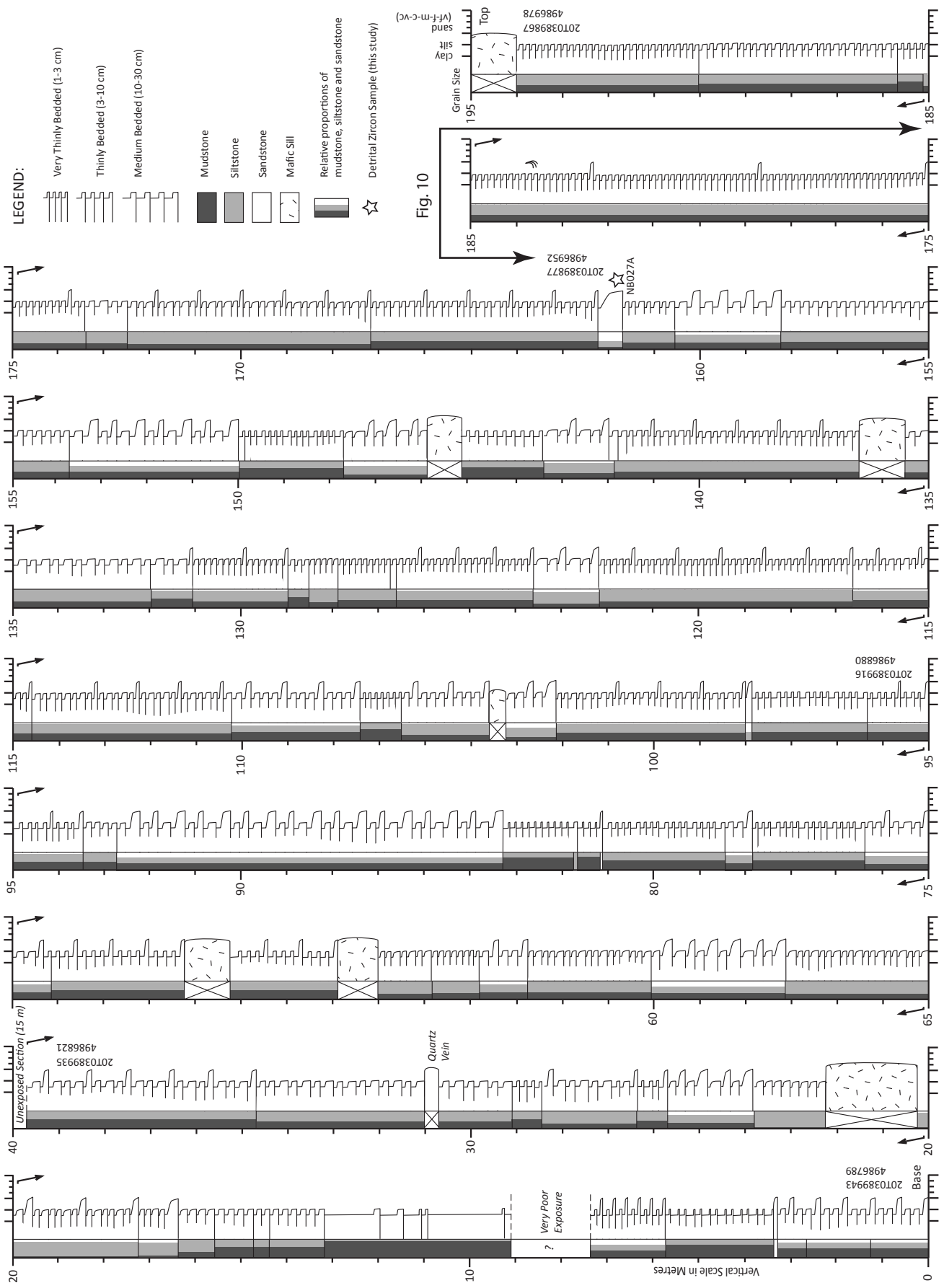

Figure 7. Generalized section of the well exposed section of the Lumsden Dam Formation type area.

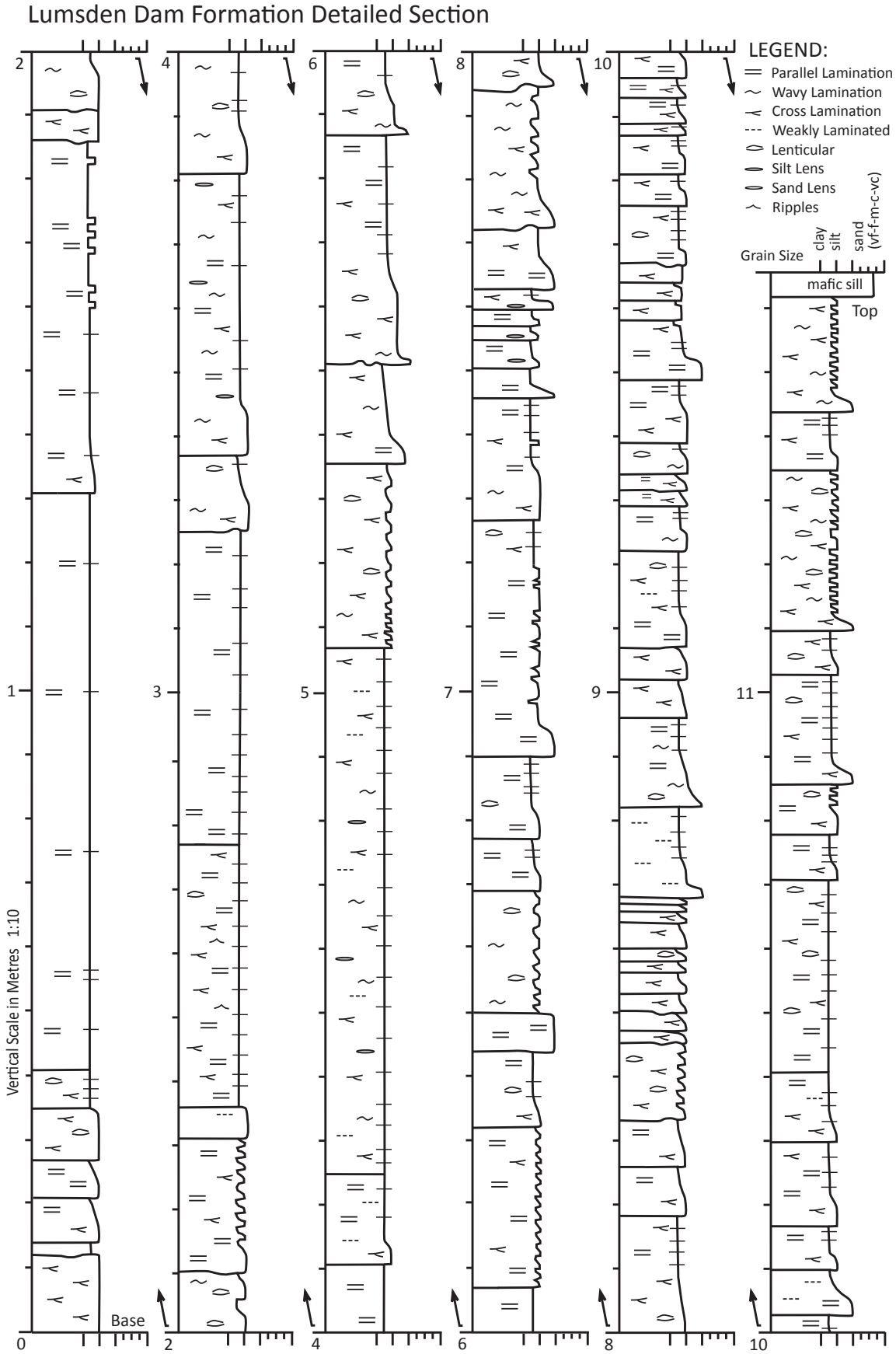

Figure 8. Detailed section representative of the Lumsden Dam Formation.

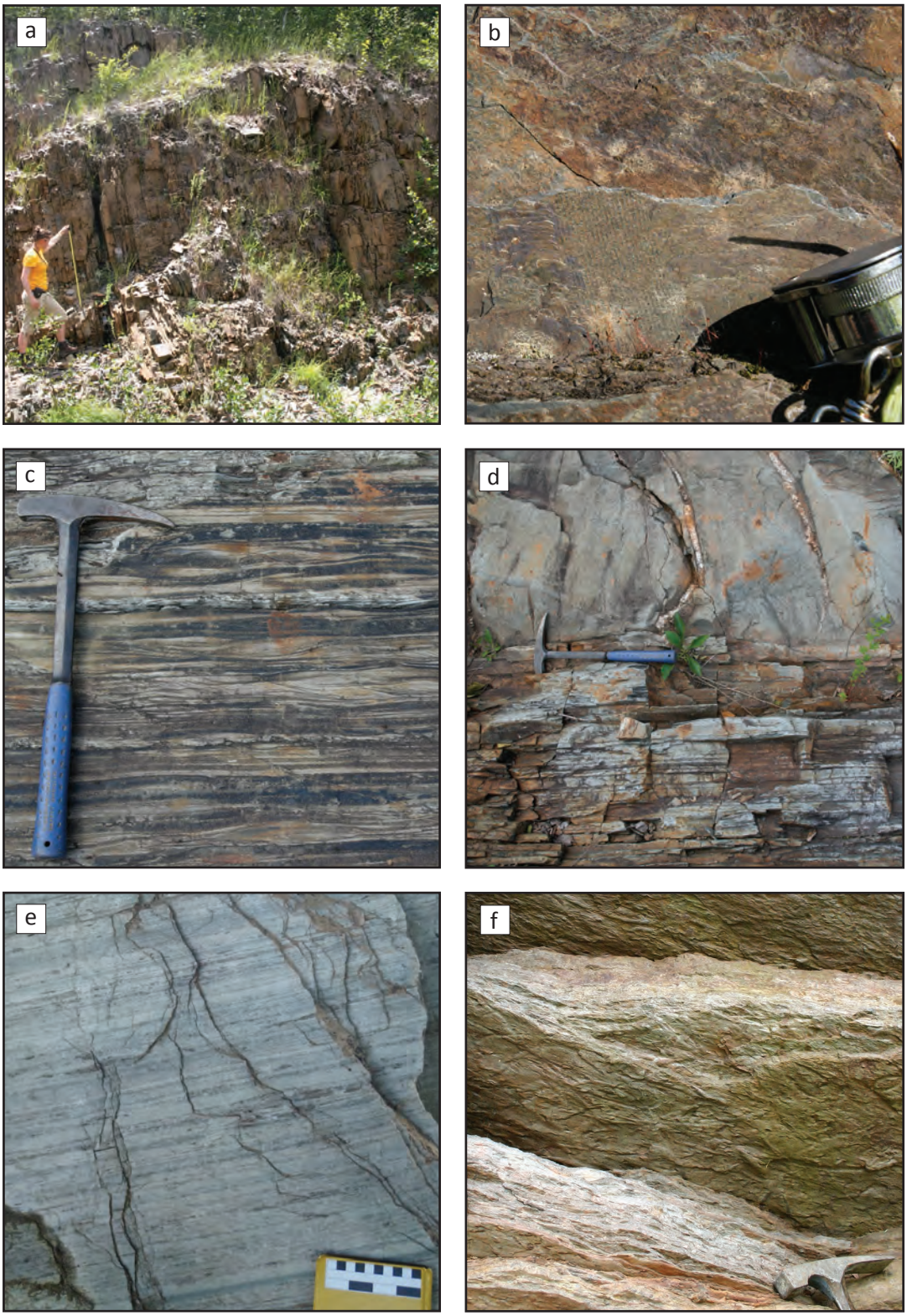

Figure 9. Typical field appearance of units in the Wolfville area: (a) Lumsden Dam Formation general view; (b) graptolite fossil in Lumsden Dam Formation, exposed on bedding surface to left of hand lens; (c) thinly interbedded siltstone and mudstone of the Lumsden Dam Formation displaying ripple cross-lamination; (d) Lumsden Dam Formation in contact with a Type I mafic sill (contact below pick of hammer); (e) finely laminated mudstone of the Elderkin Brook Formation; and (f) interbedded siltstone and mudstone of the Hellgate Falls Formation showing bioturbation structures on basal overhanging surface of bed above hammer.

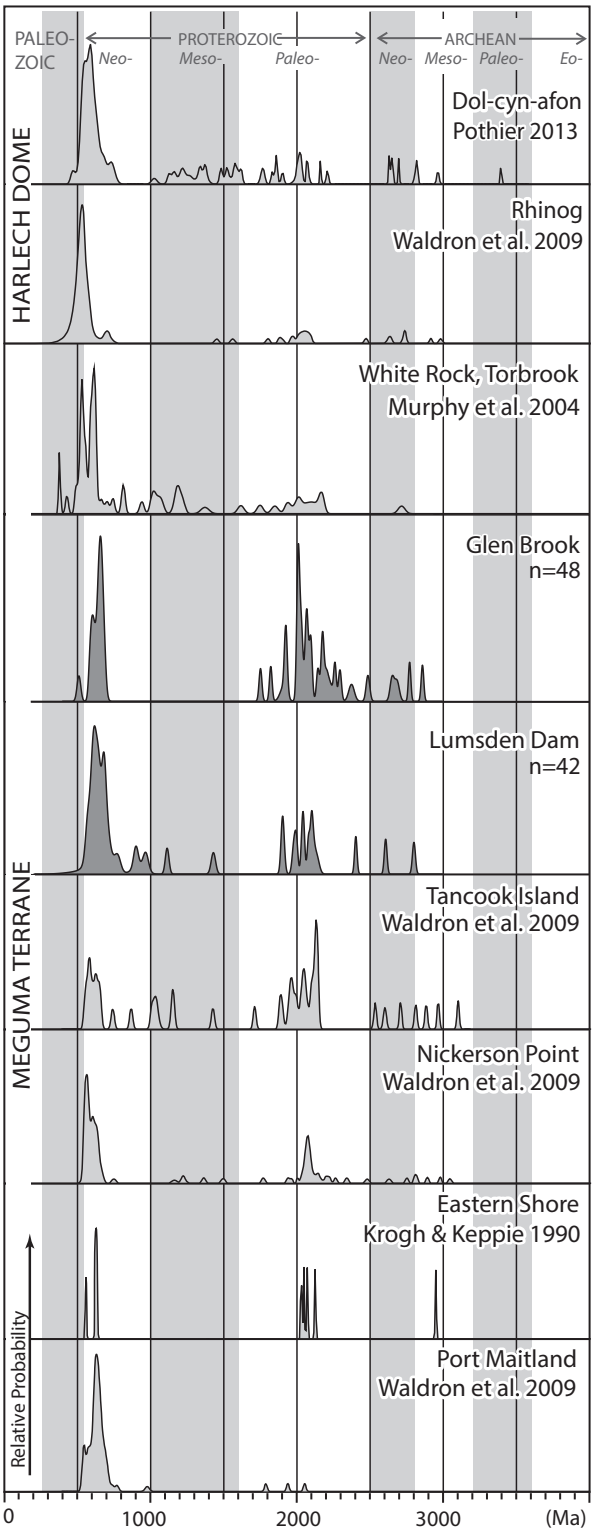

Figure 10. Probability density plot of detrital zircon data from the upper Halifax Group, compared with results from elsewhere in the Meguma terrane and the Harlech Dome region in North Wales after Krogh and Keppie (1990), Murphy *et al.* (2004a), Waldron *et al.* (2009), and Waldron *et al.* (2011). Calculations and plotting carried out with Isoplot 3.0 (Ludwig 2003). Complete analytical results and additional plots are shown in Appendices A and B.

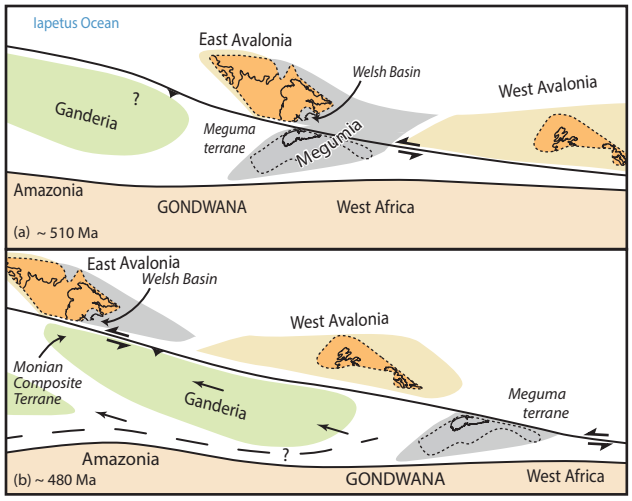

Figure 11. Possible paleogeographic reconstruction of the Gondwanan margin in (a) the Cambrian and (b) Early Ordovician, showing inferred relative displacement of Welsh basin and Meguma terrane. Dashed line in (b) schematically represents possible opening of Rheic Ocean between peri-Gondwanan terranes and Gondwana.

al. 2012).

U-PB DETRITAL ZIRCON DATING

Wolfville area

Sample NB027A for detrital zircon analysis was collected from the Lower Ordovician Lumsden Dam Formation in the overflow channel at Lumsden Dam [20T 0389877 4986952] (Fig. 1b, 2), approximately 20 m down-section from the *Rhabdinoporas flabelliformus* graptolite locality (shown at 162 m in Fig. 7). The sample was collected from a medium grey bed, 8 cm thick, of coarse siltstone. Petrographically, the sample is subarkosic wacke with subrounded grains. The rock has a primary fabric defined by the alignment of detrital mica grains and weak cleavage is detectable.

The sample was crushed using a jaw crusher and disk mill, and then passed over a Wilfley table to isolate the heavy grain fraction. Franz and heavy liquid separation were used to isolate the zircons. A random selection of zircons was mounted and imaged by electron backscatter using a scanning electron microscope. They were dated using U-Pb laser ablation multicollector inductively coupled plasma mass spectrometry (LA-MC-ICP-MS) with a Nu-Plasma instrument and UP213 laser ablation system from New Wave Research. Analytical protocol and data reduction were a modification of the procedure outlined in Simonetti *et al.* (2005). A 30 µm spot size was used except when elevated ^{206}Pb cps tripped the ion counter. When this occurred, if possible the grains were reanalyzed with a 20 µm spot size.

Two standards were used to normalize the grain ages. Standard LH94-15 with a U-Pb age of 1830 ± 1Ma is a ho-

mogeneous calc-alkaline enderbite (Simonetti *et al.* 2005; Ashton *et al.* 1999). Standard GJ-1 with a U-Pb age of 609 Ma is believed to have come from an East African pegmatite (Jackson *et al.* 2004; Elhlou *et al.* 2006). LH94-15 was used for all grains with uncorrected $^{207}Pb/^{206}Pb$ ratios greater than 0.0658, corresponding to a $^{207}Pb/^{206}Pb$ age of 800 Ma. GJ-1 was used for all grains with uncorrected $^{207}Pb/^{206}Pb$ ratios less than this value.

Minor amounts of Hg present in the argon gas supply led to slightly elevated background counts at atomic mass 204, which therefore would have yielded invalid ages if treated as common lead. Therefore, ages were not common-lead corrected unless levels of ^{204}Pb were higher than background levels (when counts per second of mass 204 were greater than 250).

One hundred and thirty-five grains were analyzed from the sample; however, 37 analyses were discarded due to low ^{206}Pb counts per second (less than 10,000), high discordance, or very low ^{238}U contents suggesting a substantial non-zircon component to the grain. Of the remaining 111 analyses, only 42 recorded ages that were between -10 and 10% discordant. For grains with $^{207}Pb/^{206}Pb$ ages older than 800 Ma the $^{207}Pb/^{206}Pb$ age is reported, as it typically shows higher analytical precision. For younger grains the $^{206}Pb/^{238}U$ age, normally more precise, is reported. The distribution of ages is shown in Figure 10. Full analytical results are reported in Appendices A and B.

The detrital zircon results for the Lumsden Dam Formation (Fig. 10 and Appendix A) show a prominent Neoproterozoic peak centered at 612 Ma, defined by a cluster of ages (24 analyses) ranging from 556 to 796 Ma (Fig. 10). This cluster is separated by a gap from an early Neoproterozoic grain group (3 analyses, 899 to 966 Ma). Two grains are of Mesoproterozoic age (1112 ± 25 and 1429 ± 30 Ma) and a significant Paleoproterozoic grain population with a cluster (9 analyses) ranges in age from ~ 1900 to 2140 Ma. The sample also contains one older Paleoproterozoic grain and two Archean grains with ages 2405 ± 17, 2610 ± 19 and 2803 ± 20 Ma.

Young grains were generally euhedral to subhedral, and many exhibited oscillatory zoning. Old grains were generally sub-rounded to rounded and showed more homogeneous internal compositions with only weak zoning. Other features present in the grain population included core-rim structures, inclusions and fractures. These features typically were correlated with discordant ages.

Eastern Nova Scotia

Additional samples were collected in the Bluestone Quarry Formation, but failed to yield sufficient zircon grains on crushing and separation for worthwhile analysis. Therefore, to supplement the Lumsden Dam sample, and to represent equivalent strata lying unequivocally southeast of the CPSZ, we present here an older data set, previously unpublished, from the laterally equivalent Glen Brook Formation (Fig. 2). This sample (LR080B, Fig. 1) was collected at a small quarry on Benvie Road [20T 498149 4997829] in Halifax Regional Municipality, from a bed of laminated siltstone approximately 15 cm thick. Zircons were extracted using the same methods as the sample from the Lumsden Dam Formation. One hundred and ten grains were analysed but, as for the Lumsden Dam sample, initial processing of the data produced many discordant results. This was probably due to the small grain size, which meant the ablated regions included zircon with variable isotopic age. Also, these analyses were subject to unusually large fluctuations in the signal at mass 204, leading to inappropriately large common-Pb corrections. On re-examination of the results, it proved possible to avoid some of the discordant results by excluding aberrant signals at the beginning or end of the ablation sequences, and by not attempting to apply the common-Pb correction; this probably resulted in the exclusion of a few analyses that contained significant common-Pb, but was more than compensated by additional concordant results from grains with little common-Pb. The reprocessed analyses contain sufficient concordant results (46 analyses) for comparison with the Lumsden Dam sample. Complete analytical results are provided in Appendix B.

The resulting distribution shows many similarities with the Lumsden Dam results, but some differences. A single grain at 511 ± 25 Ma, within error of the inferred depositional age, has no counterpart in the Lumsden Dam sample. A Neoproterozoic cluster of 15 grains ranges from ~585 to ~685 Ma. There are no Mesoproterozoic grains, but as in the case of the Lumsden Dam Formation a large Paleoproterozoic population (26 grains) is present. The range of this Paleoproterozoic population is wider (~1750 to 2490 Ma) but the largest concentration of grains is between 2000 and 2100 Ma, as in the Lumsden Dam sample. A small Archean population of 4 grains also covers approximately the same span as in the Lumsden Dam Formation.

DISCUSSION

Correlation

The Bluestone Quarry, Glen Brook, Feltzen, Bear River, and Lumsden Dam formations have been correlated based on their lithological similarities and their stratigraphic position above the Cunard Formation and its lateral equivalents, the North Alton and Acacia Brook Formations (White 2010a). The units comprise interbedded sandstone and siltstone with medium to dark grey mudstone and slate. The majority of beds exhibit vertical sequences of sedimentary structures described in the Bouma sequence (Bouma 1962), typical of turbidites. They are dominantly low-energy turbidites that record Bouma divisions Tb–Te and Tc–Te, and contain high-energy turbidites that record Bouma divisions Ta–e and Ta,e. Given these similarities, there are also important differences between the Bluestone Quarry and Lumsden Dam formations in particular. The

Bluestone Quarry Formation contains a higher proportion of high-energy turbidites (Point Pleasant Park member) than the Lumsden Dam Formation and the mass transport deposits in the Bluestone Quarry Formation (Chain Rock member) are not present in the Lumsden Dam Formation. This difference can be attributed to slightly different positions relative to the basin margin, either laterally, or basinward. The slightly coarser Bluestone Quarry Formation may have been more proximal than the Lumsden Dam Formation. This is consistent with paleocurrent data that suggest a northwestward (present-day coordinates) flow direction, with the source region to the SE and a deep basin to the NW (Schenk 1970; Waldron *et al.* 2015).

The Meguma Supergroup has been correlated with the Cambrian to Tremadocian succession in the Harlech Dome of North Wales (Waldron *et al.* 2011). Both regions record thick early Cambrian continentally derived sandstone turbidites, overlain by early to middle Cambrian alternating mud-rich and sand-rich units that are enriched in manganese. The manganiferous interval is characterized in all regions by a diverse assemblage of trace fossils, including locally abundant *Teichichnus*. Above, the succession consists of anoxic, organic-rich turbidites, shallowing upwards into paler, Tremadocian mudstone and siltstone of the Dolcyn-afon Formation. This unit has been correlated with the Bluestone Quarry and Lumsden Dam formations of the Meguma terrane (Waldron *et al.* 2011; White *et al.* 2012; Pothier *et al.* 2015) based on its age and stratigraphic position.

Age

The Lumsden Dam Formation contains the graptolite *Rhabdinopora flabelliformis flabelliformis* and an acritarch assemblage of Tremadocian age (White *et al.* 2012). No fossils have been discovered in the Bluestone Quarry Formation and attempts to extract detrital zircons were unsuccessful; hence there is still no direct evidence for its age. Its stratigraphic position above the Cunard Formation and the lithological similarities between it and the Lumsden Dam Formation suggests the Bluestone Quarry Formation was also deposited during the Tremadocian. However, it is possible that the top of the Cunard Formation (and laterally equivalent units) represents a diachronous surface.

Depositional Environment

Schenk (1983) suggested the Meguma succession was deposited along the continental embankment of a passive margin; however, whole-rock geochemical data have been interpreted to suggest deposition in an active continental margin and (or) an island arc setting, not a passive margin (White *et al.* 2006; White and Barr 2010). Waldron *et al.* (2009) proposed a rift or extensional environment that subsequently became inactive. This hypothesis helps to explain the upward transition from a relatively juvenile Avalonian and Pan-African source to an older more diverse source region. In the early stages of basin development the uplifted rift flanks would supply the only source of sediment; later thermal subsidence permitted for a more extensive source region including Proterozoic and Archean rocks. This trend is reflected in ε_{Nd} values that show a change from a restricted juvenile source to more diverse and isotopically evolved sources (Waldron *et al.* 2009). This general model also explains the rapid accumulation of the ~13 km thick succession, and perhaps the differences in the stratigraphic succession on either side of the CPSZ (Waldron *et al.* 2009).

The Goldenville Group is interpreted to represent a submarine, deep-sea fan deposit formed by turbidity currents and other types of sediment gravity flow (e.g., Schenk 1971; Harris and Schenk 1976; Waldron and Jensen 1985). Manganese accumulation at the top of the Goldenville Group was interpreted by Waldron (1992) as reflecting the intersection of the base of an oxygen minimum zone, in which Mn(II) was soluble, with the sea floor. The depositional environment for the shaly Cunard Formation of the lower Halifax Group has generally been interpreted as the mid- or upper-fan region of a muddy deep-marine fan that prograded over the Goldenville Group (Schenk 1971; Stow *et al.* 1984). Waldron (1987, 1992) attributed the abundance of graphite and sulphide minerals in the Cunard Formation to anaerobic conditions in the water column. The Lumsden Dam and Bluestone Quarry formations record a succession of low to high-energy turbidite deposits, probably deposited under slightly more oxidizing conditions, supported by the presence of trace fossils in the Feltzen and Bear River formations, inferred to be laterally equivalent. The presence of a mass transport deposit in the Bluestone Quarry Formation (Waldron *et al.* 2015) indicates that this unit was likely deposited in a slope environment. The Elderkin Brook and Hellgate Falls formations, which overlie the Lumsden Dam Formation (Fig. 2) show an upward progression into a highly bioturbated facies with abundant trace fossils, that lacks turbiditic structures. This suggests a transition from a slope into an outer shelf environment by the late Tremadocian. These observations are consistent with those of Schenk (1997), who interpreted the upper formations of the Halifax Group to represent a shoaling succession deposited between the upper slope of a prodelta and a muddy outer shelf.

Provenance and paleogeography

The Meguma terrane resided along the northern margin of Gondwana during the Cambrian (e.g., Cocks and Torsvik 2002; Nance *et al.* 2008); however, its exact position, and whether it formed its own discrete terrane or was a part of West Avalonia, are still subjects of controversy. Schenk (1970, 1981, 1997) and Robinson *et al.* (1998) have suggested the succession represents a continental prism that formed off the northwestern African margin, while others (e.g., Landing 2004; Murphy *et al.* 2004a) believed that it

formed on the margin of West Avalonia. Some would place the Meguma terrane adjacent to the Amazonian craton (e.g., Keppie 1977; Linnemann *et al.* 2012), and others closer to the West African craton (e.g., Schenk 1997; Waldron *et al.* 2009).

Geochronological analyses of detrital zircon grains in clastic sedimentary rocks offer important information about potential source regions for sedimentary basin fill. This method has been an essential tool in determining the paleogeographic positions of many peri-Gondwanan terranes. Several detrital zircon studies (e.g., Waldron *et al.* 2009; Barr *et al.* 2012) within the Meguma terrane, West Avalonia, and Ganderia have attempted to distinguish West African craton from Amazonian craton sources. The West African craton is characterized by Paleoproterozoic rocks (2.0 to 2.2 Ga) related to the Eburnean and Birimian orogens, and Archean rocks (Rocci *et al.* 1991; Lerouge *et al.* 2006). The Amazonian craton has Paleoproterozoic and Archean sources as well, but also has extensive Mesoproterozoioc crust including the Rio Negro belt (1.6 to 1.8 Ga) and the Rondonia-Sunsas belts (1.3 to 1.0 Ga) (Litherland *et al.* 1985; Rowley and Pindell 1989). Thus the lack of a Mesoproterozoic grain population (c. 800 to 1700 Ma) has been considered an indicator of West African rather than Amazonian provenance (e.g., Nance and Murphy 1996; Linnemann *et al.* 2004).

Several detrital zircon samples have been analyzed from the Goldenville and Rockville Notch groups (Krogh and Keppie 1990; Murphy *et al.* 2004b; Waldron *et al.* 2009) (Fig. 10). Units sampled low in the Goldenville Group show a restricted distribution with prominent late Neoproterozoic grain populations. A Neoproterozoic to early Cambrian peak is common to many peri-Gondwanan terranes including Avalonia (Barr *et al.* 2012) and Ganderia (Fyffe *et al.* 2009; Murphy *et al.* 2004b; Waldron *et al.* 2011) and reflects Avalonian / Pan-African events that occurred between c. 540 and 700 Ma along the Gondwanan margin (Nance *et al.* 1991, 2008).

Samples from higher in the Goldenville Group contain a few Mesoproterozoic grains, a significant population of grains between 2.0 and 2.2 Ga, and a range of Archean grains. These ages were interpreted by Krogh and Keppie (1990) and Waldron *et al.* (2009) to indicate sources in West Africa. The detrital zircon samples collected from the Lumsden Dam and Glen Brook formations show very similar distributions to the sample from the Government Point Formation in the upper part of the Goldenville Group (Fig. 10). In addition to the late Neoproterozoic peak they also contain significant populations between 1.9 and 2.1 Ga, as well as 2.6 to 2.8 Ga Archean grains. Mesoproterozoic grains are scarce in the Lumsden Dam Formation and absent from the sample of the Glen Brook Formation. The West African source interpreted for the Goldenville Group (e.g., Waldron *et al.* 2009; Krogh and Keppie 1990) thus appears to have continued to supply detritus to the Meguma terrane into the Ordovician.

Relationship to the Welsh basin

The sedimentary rocks of the Meguma terrane have been correlated with those of the Harlech Dome in North Wales (Waldron *et al.* 2011), leading to the inclusion of both terranes in the domain Megumia. Both regions display thick early Cambrian (Cambrian Series 1-2) continentally derived sandstone turbidites, overlain by early to middle (Series 2-3) Cambrian alternating mud-rich and sand-rich units in which manganese is concentrated. Above, the successions both comprise anoxic, organic-rich turbidites of Furongian (Cambrian Series 4) age, shallowing upward into paler, Early Ordovician mudstone and siltstone that contain the graptolite *Rhabdinopora flabelliformis flabelliformis.* In the Harlech Dome, the Tremadocian is represented by the mudstone-rich Dol-cyn-afon Formation which has previously been compared to the Lumsden Dam Formation based on its age and fossil assemblage (Waldron *et al.* 2011; White *et al.* 2012).

By the late Tremadocian the stratigraphic similarity between the Welsh Basin and the Meguma terrane ends and their histories diverged. The Lumsden Dam Formation records slope conditions that transition into shelf sedimentation recorded in the Elderkin Brook and Hellgate Falls formations. This was followed by a period of non-deposition and/or erosion and then by deposition of the Silurian volcano-sedimentary succession of the Rockville Notch Group. In the Harlech Dome, the Dol-cyn-afon Formation is unconformably overlain by late Tremadocian volcanic rocks followed by Floian sandstones and back-arc volcanic rocks through to the Late Ordovician.

Detrital zircon samples collected from Cambrian rocks (Rhinog and Gamlan formations) in the Harlech Dome exhibit a similar distribution (Fig. 10) to the Cambrian rocks of the Goldenville Group indicating they too were likely sourced from the Pan-African – Avalonian orogen and the West African craton (Waldron *et al.* 2011; Pothier *et al.* 2014). In contrast, new results from the Dol-cyn-afon Formation (Pothier *et al.* 2014) exhibit a detrital zircon distribution interpreted to show input of sediment from the Monian Composite terrane (Fig. 1a) in North Wales, which has been correlated with Ganderia of Atlantic Canada (Collins and Buchan 2004).

The similarities between the Dol-cyn-afon Formation and Monian detrital zircon distributions indicate the juxtaposition of the Monian composite terrane with North Wales by the Tremadocian (Pothier *et al.* 2014) along the NE-SW striking Menai Strait Fault System, which represents a terrane boundary in North Wales (Gibbons 1987). The new observations presented here are consistent with the divergence in Ordovician histories between the two basins and suggest that, if the two basins were contiguous in the Cambrian period, they had parted by the Tremadocian.

Waldron *et al.* (2011) proposed two paleogeographic reconstructions that would allow the Meguma terrane and the Welsh Basin to be adjacent during the Cambrian. In

these scenarios, a likely mechanism to accommodate their diverging Ordovician histories would be strike-slip movement; Neoproterozoic subduction and arc activity along the Gondwanan margin were succeeded by a more stable environment by the early Paleozoic, where sinistral transcurrent motion is thought to have been prevalent (Nance *et al.* 1991, 2008). The Menai Strait Fault System between the Monian composite terrane and Welsh basin, active between the early Cambrian and late Carboniferous, is interpreted to show sinistral transpression (Gibbons 1987; Gibbons and Horák 1990). If a continuation of this fault system were to pass through Megumia, left-lateral migration could have displaced the Welsh Basin from an original position next to the Meguma terrane and juxtaposed it with the Monian composite terrane along the Gondwana margin. Figure 11 shows a possible terrane configuration consistent with this hypothesis, based on the assumption that Megumia was located within a rift system between East and West Avalonia. This model is consistent with both the sinistral transpressional setting for the Menai Strait Fault System, with the likely initial position of Ganderia (e.g., Pollock *et al.* 2009; van Staal *et al.* 2012) along the Amazonian margin, and with substantial rotation of portions of Avalonia during later Paleozoic history as suggested by Vizan *et al.* (2003).

CONCLUSIONS

(1) The Lumsden Dam Formation and Bluestone Quarry Formation are defined as formal lithostratigraphic units within the Halifax Group.

(2) The Bluestone Quarry and Lumsden Dam formations represent slope-related environments.

(3) The detrital zircon results from the Lumsden Dam Formation and Glen Brook Formation (likely correlative with the Bluestone Quarry Formation) show similar results to the Government Point Formation in the upper part of the Goldenville Group.

(4) These age populations are consistent with a source region in the West African craton with possible minor input from the Amazonian craton.

(5) Although the age and depositional environment for the Lumsden Dam Formation and the Dol-cyn-afon Formation of the Harlech Dome are similar, their different detrital zircon age populations suggest that the histories of the basins had diverged by the Tremadocian.

(6) A possible explanation for the diversification in detrital zircon ages within the Harlech Dome succession, and the diverging histories of the Meguma terrane and North Wales, could be left-lateral relative movement parallel to the margin of Gondwana along a transpressional fault system that separated the once adjacent basins by the Floian.

ACKNOWLEDGEMENTS

C.E.White publishes with the permission of the Director of the Nova Scotia Department of Natural Resources. We are grateful to the Natural Sciences and Engineering Research Council for Discovery Grant (A8508) funding to J.W.F. Waldron, and to the University of Alberta for student support to H.D. Pothier. Maryam Dzulkefli and Morgan Snyder assisted in the field. Guangchen Chen provided technical support in the mass spectrometry laboratory and Heather Clough, Matthew Kliffer and Robert Dokken assisted with mineral separation. We are grateful to journal referees Les Fyffe and Rob Raeside for their insightful reviews, and to the journal editors for discussions about formal and informal nomenclature.

REFERENCES

Ashton, K.E., Heaman, L.M., Lewry, J.F., Hartlaub, R.P., and Shi, R. 1999. Age and origin of the Jan Lake Complex: a glimpse at the buried Archean craton of the Trans-Hudson Orogen. Canadian Journal of Earth Sciences, 36, pp. 185–208. http://dx.doi.org/10.1139/e98-038

Barr, S.M., Hamilton, M.A., Samson, S.D., Satkoski, A.M., and White, C.E. 2012. Provenance variations in northern Appalachian Avalonia based on detrital zircon age patterns in Ediacaran and Cambrian sedimentary rocks, New Brunswick and Nova Scotia, Canada. Canadian Journal of Earth Sciences, 49, pp. 533–546. http://dx.doi.org/10.1139/e11-070

Boggs, S., 2001. Principles of sedimentology and stratigraphy 3rd edition Prentice-Hall, Upper Saddle River, New Jersey, 726 p.

Bouma, A.H. 1962. Sedimentology of some Flysch Deposits. A Graphic Approach to Facies Interpretation Elsevier, Amsterdam 168 p.

Bouyx, E., Blaise, J., Brice, D., Degardin, J.M., Goujet, D., Gourvennec, R., Le Menn, J., Lardeux, H., Morzadec, P. and Paris, F. 1997. Biostratigraphie et paleobiogeographie du Siluro-Devonien de la zone de Meguma (Nouvelle-Écosse, Canada). Canadian Journal of Earth Sciences, 34, pp. 1295–1309. http://dx.doi.org/10.1139/e17-103

Cardwell, D.H., Erwin, R.B., and Woodward, H.P. 1968. Geologic Map of West Virginia: West Virginia Geological and Economic Survey, Map 1, East Sheet, scale 1:250 000.

Clarke, D.B. and Halliday, A.N. 1980. Strontium isotope geology of the South Mountain batholith, Nova Scotia. Geochimica et Cosmochimica Acta, 44, pp. 1045–1058. http://dx.doi.org/10.1016/0016-7037(80)90058-7

Clarke, D.B., Halliday, A.N., and Hamilton, P.J. 1988. Neodymium and strontium isotopic constraints on the origin of the peraluminous granitoids of the South Mountain Batholith, Nova Scotia, Canada. Chemical Geology, 73, pp. 15–24.

Cocks, L.R.M. and Torsvik, T.H. 2002. Earth geography from 500 to 400 million years ago: a faunal and palaeomagnetic review. Journal of the Geological Society, London, 159, pp. 631–644. http://dx.doi.org/10.1144/0016-764901-118

Collins, A.S. and Buchan, C. 2004. Provenance and age constraints of the South Stack Group, Anglesey, UK: U-Pb SIMS detrital zircon data. Journal of the Geological Society, London, 161, pp. 743–746. http://dx.doi.org/10.1144/0016-764904-036

Eberz, G.W., Clarke, D.B., Chatterjee, A.K., and Giles, P.S. 1991. Chemical and isotopic composition of the lower crust beneath the Meguma Lithotectonic Zone, Nova Scotia: Evidence from granulite facies xenoliths. Contributions to Mineralogy and Petrology, 109, pp. 69–88. http://dx.doi.org/10.1007/BF00687201

Elhlou, S., Belousova, E., Griffin, W.L., Pearson, N.J., and O'Reilly, S.Y. 2006. Trace element and isotopic composition of GJ-red zircon standard by laser ablation. Geochimica et Cosmochimica Acta, 70, pp. A158–A158. http://dx.doi.org/10.1016/j.gca.2006.06.1383

Fyffe, L.R., Barr, S.M., Johnson, S.C., McLeod, M.J., McNicoll, V.J., Valverde-Vaquero, P., van Staal, C.R., and White, C.E. 2009. Detrital zircon ages from Neoproterozoic and Early Paleozoic conglomerate and sandstone units of New Brunswick and coastal Maine: Implications for the tectonic evolution of Gander-ia. Atlantic Geology, 45, pp. 110–144. http://dx.doi.org/10.4138/atlgeol.2009.006

Gibbons, W. 1987. Menai Strait fault system: An early Caledonian terrane boundary in north Wales. Geology, 15, pp. 744–747. http://dx.doi.org/10.1130/0091-7613(1987)15<744:MSFSAE>2.0.CO;2

Gibbons, W. and Horák, J. 1990. Contrasting metamorphic terranes in northwest Wales. Geological Society, London, Special Publications, 51, pp. 315–327. http://dx.doi.org/10.1144/GSL.SP.1990.051.01.20

Gingras, M.K., Waldron, J.W.F., White, C.E., and Barr, S.M. 2011. The evolutionary significance of a Lower Cambrian trace-fossil assemblage from the Meguma terrane, Nova Scotia. Canadian Journal of Earth Sciences, 48, pp. 71–85. http://dx.doi.org/10.1139/E10-086

Greenough, J.D., Krogh, T.E., Kamo, S.L., Owen, J.V., and Ruffman, A. 1999. Precise U-Pb dating of Meguma basement xenoliths: new evidence for Avalonian underthrusting. Canadian Journal of Earth Sciences, 36, pp. 15–22. http://dx.doi.org/10.1139/e98-079

Harris, I.M. and Schenk P.E. 1976. The Meguma Group. Maritime Sediments, 11, pp. 25–46.

Hart, G.G. 2006. Andalusite in the South Mountain Batholith contact aureole, Halifax Nova Scotia: a tale of two isograds. Unpublished B.Sc. thesis, Dalhousie University, Halifax, Nova Scotia, 121 p.

Hibbard, J.P., van Staal, C.R., Rankin, D.W., and Williams, H. 2006.Lithotectonic map of the Appalachian orogen, Canada — United States of America. Geological Survey of Canada Map 02096A, scale 1:1 500 000.

Horne, R.J. and Pelley, D. 2007. Geological transect of the Meguma terrane from Centre Musquodoboit to Tangier. *In* Mineral Resources Branch, Review of Activities 2006. *Edited by* D.R. MacDonald. Nova Scotia Department of Natural Resources, Report, ME 2007-1. pp. 71–89.

Jackson, S.E., Pearson, N.J., Griffin, L., and Belousova, E.A. 2004. The application of laser ablation-inductively coupled plasma-mass spectrometry to in situ U-Pb zircon geochronology, 211, pp. 47–69.

Jamieson, R.A., Tobey, N., and ERTH 3020. 2005. Contact metamorphism of the Halifax Formation on the southeastern margin of the Halifax Pluton, Halifax, Nova Scotia. GAC-MAC-CSPG-CSSS Joint Annual Meeting, Halifax, Nova Scotia, Abstract Volume, 30, p. 95.

Jamieson, R.A., Waldron, J.W.F., and White, C.E. 2011. Bluestone formation of the Halifax Group: metamorphosed slope and mass-transport deposits, Halifax Peninsula, Nova Scotia. Atlantic Geology, 47, pp. 24–25.

Jamieson, R.A., Hart, G.G., Chapman, G.G., and Tobey, N.W. 2012. The contact aureole of the South Mountain Batholith in Halifax, Nova Scotia: geology, mineral assemblages, and isograds. Canadian Journal of Earth Sciences, 49, pp. 1280–1296. http://dx.doi.org/10.1139/e2012-058

Keppie, J.D. 1977. Tectonics of Southern Nova Scotia. Nova Scotia Department of Mines Paper 77-1, 34 p.

Keppie, J.D. and Dallmeyer, R.D. 1987. Dating transcurrent terrane accretion: an example from the Meguma and Avalon Composite terranes in the Northern Appalachians. Tectonics, 6, pp. 831–847. http://dx.doi.org/10.1029/TC006i006p00831

Keppie, J.D. and Krogh, T.E. 1999. U-Pb Geochronology of Devonian Granites in the Meguma Terrane of Nova Scotia, Canada: Evidence for Hotspot Melting of a Neoproterozoic Source. The Journal of Geology, 107, pp. 555–568. http://dx.doi.org/10.1086/314369

Keppie, J.D. and Krogh, T.E. 2000. 440 Ma igneous activity in the Meguma Terrane, Nova Scotia, Canada: part of the Appalachian overstep sequence. American Journal of Science, 300, pp. 528–538. http://dx.doi.org/10.2475/ajs.300.6.528

Keppie, J.D. and Muecke, G.K. 1979. Metamorphic Map of Nova Scotia. Nova Scotia Department of Mines and Energy, Map ME 1979-006, scale 1:2 000 000.

Keppie, J.D., Dostal, J., Murphy, J.B., and Cousens, B.L. 1997. Palaeozoic withinplate volcanic rocks in Nova Scotia reinterpreted: isotopic constraints on magmatic source and palaeocontinental reconstructions. Geological Magazine, 134, pp. 425–447. http://dx.doi.org/10.1017/S001675689700719X

Klein, G.D. 1962. Triassic sedimentation, Maritime Provinces, Canada. Geological Society of America Bulletin. 73, pp. 1127–1146. http://dx.doi.org/10.1130/0016-7606(1962)73[1127:TSMPC]2.0.CO;2

Krogh, T.E. and Keppie, J.D. 1990. Age of detrital zircon and titanite in the Meguma Group, southern Nova Scotia, Canada: Clues to the origin of the Meguma Terrane. Tectonophysics, 177, pp. 307–323. http://dx.doi.org/10.1016/0040-1951(90)90287-I

Landing, E. 2004. Precambrian-Cambrian boundary interval deposition and marginal platform of the Avalon microcontinent. Journal of Geodynamics, 37, pp. 411–435. http://dx.doi.org/10.1016/j.jog.2004.02.014

Lane, T.E. 1975. Stratigraphy of the White Rock Formation. Maritime Sediments, 11, pp. 87–106.

Lerouge, C., Cocheria, A., Toteu, S.F., Penaye, J., Milesi, J.P., Tchameni, R., Nsifa, E.N., Fanning, C.M., and Deloule, E. 2006. Shrimp U–Pb zircon age evidence for Paleoproterozoic sedimentation and 2.05Ga syntectonic plutonism in the Nyong Group, South-Western Cameroon: consequences for the Eburnean–Transamazonian belt of NE Brazil and Central Africa. Journal of African Earth Sciences, 44, pp. 413–427. http://dx.doi.org/10.1016/j.jafrearsci.2005.11.010

Linnemann, U., McNaughton, N.J., Romer, R.L., Gehmlich, M., Drost, K., and Tonk, C. 2004. West African provenance for Saxo-Thuringia (Bohemian Massif): Did Armorica ever leave pre-Pangean Gondwana? U/Pb-SHRIMP zircon evidence and the Nd-isotopic record. International Journal of Earth Sciences, 93, pp. 683–705. http://dx.doi.org/10.1007/s00531-004-0413-8

Linnemann, U., Herbosch, A., Liegeois, J.P., Pin, C., Gartner, A., and Hofmann, M. 2012. The Cambrian to Devonian odyssey of the Brabant Massif within Avalonia: A review with new zircon ages, geochemistry, Sm–Nd isotopes, stratigraphy and palaeogeography. Earth-Science Reviews, 112, pp. 126–154. http://dx.doi.org/10.1016/j.earscirev.2012.02.007

Litherland, M., Klinck, B.A., O'Connor, E.A., and Pitfield, P.E.J. 1985. Andean-trending mobile belts in the Brazilian Shield. Nature, 314, pp. 345–348. http://dx.doi.org/10.1038/314345a0

Ludwig, K.R. 2003. User's Manual for Isoplot 3.00. Berkeley Geochronology Center Special Publication, 4. 74 p.

MacDonald, L.A., Barr, S.M., White, C.E., and Ketchum, J.W.F. 2002. Petrology, age, and tectonic setting of the White Rock Formation, Meguma terrane, Nova Scotia: evidence for Silurian continental rifting. Canadian Journal of Earth Sciences, 39, pp. 259–277. http://dx.doi.org/10.1139/e01-074

Martel, A.T. and McGregor, D.C. 1993. Stratigraphic significance of Upper Devonian and Lower Carboniferous miospores from the type area of the Horton Group, Nova Scotia. Canadian Journal of Earth Science. 30, pp. 1091–1098. http://dx.doi.org/10.1139/e93-092

Murphy, J.B., Fernandez-Suarez, J., Keppie, J.D., and Jeffries, T.E. 2004a. Contiguous rather than discrete Paleozoic histories for the Avalon and Meguma Terranes based on detrital zircon data. Geology, 32, pp. 585–588. http://dx.doi.org/10.1130/G20351.1

Murphy, J.B., Fernandez-Suarez, J., Jeffries, T.E., and Strachan, R.A. 2004b. U-Pb (LA-ICP-M.S.) dating of detrital zircons from Cambrian clastic rocks in Avalonia: erosion of a Neoproterozoic arc along the northern Gondwanan margin. Journal of the Geological Society, London, 161, pp. 243–254. http://dx.doi.org/10.1144/0016-764903-064

Nance, R.D. and Murphy, J.B. 1996. Basement isotopic signatures and Neoproterozoic paleogeography of Avalonian–Cadomian and related terranes in the Circum-North Atlantic. *In* Avalonian and Related Peri-Gondwanan Terranes of the Circum-North Atlantic. *Edited by* R.D. Nance and M.D. Thompson. Geological Society of America, Special Papers, 304, pp. 333–346. http://dx.doi.org/10.1130/0-8137-2304-3.333

Nance, R.D., Murphy, J.B., Strahan, R.A., D'Lemos, R.S., and Taylor, G.K. 1991. Late Preoterozoic tectonostratigraphic evolution of the Avalonian and Cadomian terranes. Precambrian Research, 53, pp. 41–78. http://dx.doi.org/10.1016/0301-9268(91)90005-U

Nance, R.D., Murphy, J.B., Strachan, R.A., Keppie, D.J. Gutiérrez-Alonso, G., Fernández-Suárez, J., Quesada, C., Linnemann, U., D'lemos, R., and Pisarevsky, S.A. 2008. Neoproterozoic-early Palaeozoic tectonostratigraphy and palaeogeography of the peri-Gondwanan terranes: Amazonian v. West African connections. Geological Society, London, Special Publications, 297, pp. 345–383.

O'Brien, B.H. 1988. A Study of the Meguma Terrane in Lunenburg County, Nova Scotia. Geological Survey of Canada Open File, 1823, 139 p. http://dx.doi.org/10.4095/130496

Peng, S., Babcock, L.E., and Cooper, R.A. 2012. The Cambrian Period. *In* A Geologic Time Scale 2012. *Edited by* F.M. Gradstein, J.G. Ogg, M. Schmitz, and G. Ogg. Elsevier, Amsterdam, pp. 437–488. http://dx.doi.org/10.1016/B978-0-444-59425-9.00019-6

Pollock, J.C., Hibbard, J.P., and Sylvester, P.J. 2009. Early Ordovician rifting of Avalonia and birth of the Rheic Ocean: U–Pb detrital zircon constraints from Newfoundland. Journal of the Geological Society, London, 166, pp. 501–515. http://dx.doi.org/10.1144/0016-76492008-088

Pothier, H.D. 2013. Cambrian-Ordovician successions and detrital zircon geochronology of North Wales and Nova Scotia: terrane interactions between Ganderia and Megumia. Unpublished M.Sc. thesis, University of Alberta, Edmonton, Alberta, 183 p.

Pothier, H. D., Waldron, J.W.F., Schofield, D.I., and Dufrane S.A. 2014. Peri-Gondwanan terrane interactions recorded in the Cambrian-Ordovician detrital zircon geochronology of North Wales. Gondwana Research, in press-corrected proof. http://dx.doi.org/10.1016/j.gr.2014.08.009

Pratt, B.R. and Waldron, J.W.F. 1991. A Middle Cambrian trilobite faunule from the Meguma Group of Nova

Scotia. Canadian Journal of Earth Sciences, 28, pp. 1843–1853. http://dx.doi.org/10.1139/e91-164

Raeside, R.P. and Jamieson, R.A. 1992. Low-pressure metamorphism of the Meguma Terrane, Nova Scotia. Geological Association of Canada and Mineralogical Association of Canada Joint Annual Meeting, Field Trip C5, Guidebook, 25 p.

Robinson, P., Tucker, R.D., Bradley, D., Berry, H.N.V., and Osberg, P.H. 1998. Paleozoic orogens in New England, USA: Geologiska Föreningens Förhandlingar, 120, pp. 119–148.

Rocci, G., Bronner, G., and Deschamps, M. 1991. Crystalline basement of the West African Craton. *In* The West African Orogens and Circum-Atlantic Correlatives. *Edited by* R.D. Dallmeyer and J.P. Lecorche. Berlin, Springer, pp. 31–61. http://dx.doi.org/10.1007/978-3-642-84153-8_3

Rowley, D.B. and Pindell, J.L. 1989. End Paleozoic–early Mesozoic western Pangean reconstruction and its implications for the distribution of Precambrian and Paleozoic rocks around Meso-America: Precambrian Research, 42, pp. 411–444. http://dx.doi.org/10.1016/0301-9268(89)90022-3

Schenk, P.E. 1970. Regional variation of the flysch-like Meguma Group (Lower Palaeozoic) of Nova Scotia, compared to recent sedimentation off the Scotian shelf. Geological Association of Canada, Special Paper 7, 127–53.

Schenk, P.E. 1971. Southeastern Atlantic Canada, northwestern Africa, and continental drift. Canadian Journal of Earth Sciences, 8, pp. 1218–1251. http://dx.doi.org/10.1139/e71-113

Schenk, P.E. 1981. The Meguma zone of Nova Scotia: a remnant of western Europe, South America or Africa? *In* Geology of North Atlantic borderlands. *Edited by* J.M Kerr, A.J. Ferguson, and L.C. Machan. Canadian Society of Petroleum Geologists, Memoir 7, pp. 119–148.

Schenk, P.E. 1983. The Meguma terrane of Nova Scotia, Canada - An aid in trans-Atlantic correlation. *In* Regional trends in the geology of the Appalachian-Caledonian-Hercynian-Mauritanide orogen. *Edited by* P.E. Schenk. D. Reidel Publishing Co., pp. 121–130.

Schenk, P.E. 1995a. Meguma Zone. *In* Chapter 3 Geology of the Appalachian-Caledonian Orogen in Canada and Greenland. *Edited by* H. Williams. Geological Survey of Canada, Geology of Canada, 6, pp. 261–277.

Schenk, P.E. 1995b. Annapolis Belt. In Chapter 4 Geology of the Appalachian-Caledonian Orogen in Canada and Greenland. Edited by H. Williams. Geological Survey of Canada, Geology of Canada, 6, pp. 367–383.

Schenk, P.E. 1997. Sequence stratigraphy and provenance on Gondwana's margin: the Meguma Zone (Cambrian to Devonian) of Nova Scotia, Canada. Geological Society of America Bulletin, 109, pp. 395–409. http://dx.doi.org/10.1130/0016-7606(1997)109<0395:SSAPOG>2.3.CO;2

Simonetti, A., Heaman, L.M., Hartlaub, R.P., Creaser, R.A., MacHattie, T.G., and Bohm, C. 2005. U-Pb zircon dating by laser ablation-MC-ICP-MS using a new multiple ion counting Faraday collector array. Journal of Analytical Atomic Spectrometry, 20, pp. 677–686. http://dx.doi.org/10.1039/b504465k

Smitheringale, W.G. 1960. Geology of the Nictaux-Torbrook map-area, Annapolis and Kings counties, Nova Scotia. Geological Survey of Canada, Paper 60-13, 32 p. http://dx.doi.org/10.4095/108628

Smitheringale, W.G. 1973. Geology of parts of Digby, Bridgetown, and Gaspereau map-areas, Nova Scotia: Geological Survey of Canada Memoir 375, 78 p. http://dx.doi.org/10.4095/109067

Stevenson, I.M. 1959. Shubenacadie and Kennetcook map areas, Colchester, Hants, and Halifax counties, Nova Scotia. Geological Survey of Canada Memoir 302, 88 p.

Stow, D.A.V., Alam, M., and Piper, D.J.W. 1984. Sedimentology of the Halifax Formation, Nova Scotia: Lower Paleozoic fine-grained turbitites. *In* Fine grained sediments: deep water processes and facies. *Edited by* D.J.W. Piper and D.A.V. Stow. Geological Society of London, Special Publication 15, pp. 127–144.

Taylor, F.C. 1965. Silurian stratigraphy and Ordovician-Silurian relationships in southwestern Nova Scotia. Geological Survey of Canada, Department of Mines and Technical Surveys, Paper 64-13, 25 p.

van Staal, C.R. 2007. Pre-Carboniferous tectonic evolution and metallogeny of the Canadian Appalachians. *In* Mineral Resources of Canada: A Synthesis of Major Deposit Types, Distinct Metallogeny, the Evolution of Geological Provinces, and Exploration Methods. *Edited by* W.D. Goodfellow. Geological Association of Canada, Mineral Deposits Division, Special Publication 5, pp. 793–818.

van Staal, C.R., Barr, S.B., and Murphy, J.B. 2012. Provenance and Tectonic Evolution of Ganderia: Constraints on the Evolution of the Iapetus and Rheic Oceans. Geology, 40, pp. 987–990. http://dx.doi.org/10.1130/G33302.1

Vizan, H., Carney, J.N., Turner, P., Ixer, R.A., Tomasso, M., Mullen, R.P., and Clarke, P. 2003. Late Neoproterozoic to Early Palaeozoic palaeogeography of Avalonia: some palaeomagnetic constraints from Nuneaton, central England. Geological Magazine, 140, pp. 685–705. http://dx.doi.org/10.1017/S001675680300832X

Waldron, J.W.F. 1987. Sedimentology of the Goldenville-Halifax transition in the Tancook Island area, South Shore, Nova Scotia. Geological Survey of Canada, Open File Report 1525., 49 p.

Waldron, J.W.F. 1992. The Goldenville–Halifax transition, Mahone Bay, Nova Scotia: relative sea-level rise in the Meguma source terrane. Canadian Journal of Earth Sciences, 29, pp. 1091–1105. http://dx.doi.org/10.1139/e92-087

Waldron, J.W.F. and Jensen, L.R. 1985. Sedimentology of the Goldenville Formation, Eastern Shore, Nova Scotia. Geological Survey of Canada, Paper, 85-15, 31 p.

Waldron, J.W.F., Piper, D.J.W., and Pe-Piper, G. 1989. Deformation of the Cape Chignecto Pluton, Cobequid Highlands, Nova Scotia: thrusting at the Meguma-Avalon boundary. Atlantic Geology, 25, pp. 51–62.

Waldron, J.W.F., White, C.E., Barr, S.M., Simonetti, A., and Heaman, L.M. 2009. Provenance of the Meguma terrane, Nova Scotia: rifted margin of early Paleozoic Gondwana. Canadian Journal of Earth Sciences, 46, pp. 1–9. http://dx.doi.org/10.1139/E09-004

Waldron, J.W.F., Schofield, D.I., White, C.E., and Barr, S.M. 2011. Cambrian successions of the Meguma Terrane, Nova Scotia, and Harlech Dome, North Wales: dispersed fragments of a peri-Gondwanan basin? Journal of the Geological Society, London, 168, pp. 83–98. http://dx.doi.org/10.1144/0016-76492010-068

Waldron, J.W.F., Jamieson R.A., Pothier H.D. and White C.E. 2015. Sedimentary and tectonic setting of a mass-transport slope deposit in the Halifax Group, Halifax Peninsula, Nova Scotia. Atlantic Geology, 51

White, C.E. 2010a. Pre-Carboniferous bedrock geology of the Annapolis Valley area (NTS 21A/14, 15, and 16; 21H/01 and 02), southern Nova Scotia. *In* Mineral Resources Branch, Report of Activities 2009. *Edited by* D.R. MacDonald. Nova Scotia Department of Natural Resources, Report 2010-1, pp. 137–155.

White, C.E. 2010b. Stratigraphy of the Lower Paleozoic Goldenville and Halifax groups in the western part of southern Nova Scotia. Atlantic Geology, 46, pp. 136–154. http://dx.doi.org/10.4138/atlgeol.2010.008

White, C.E. and Barr, S.M. 2010. Petrochemistry of the Lower Paleozoic Goldenville and Halifax groups, southwestern Nova Scotia, Canada: implications for stratigraphy, provenance, and tectonic setting of Meguma. *In* From Rodinia to Pangea: The Lithotectonic Record of the Appalachian Region. Geological Society of America Memoir 206, pp. 347–366.

White, C.E., Barr, S.M., and Toole, R.M. 2006. New insights on the origin of the Meguma Group in southwestern Nova Scotia, Canada. Nova Scotia Department of Natural Resources, Mineral Resource Branch, Open File Illustration, ME 2006-2.

White, C.E., Barr, S.M., Horne, R.J., and Hamilton, M.A. 2007. The Neoacadian orogeny in the Meguma terrane, Nova Scotia, Canada. *In* 42nd Annual Meeting Geological Society of America, Northeastern Section, March 12-14, Abstracts with Programs, 39, p. 69.

White, C.E., Bell, J.A., McLeish, D.F., Macdonald, M.A., Goodwin, T.A., and MacNeil, J.D. 2008. Geology of the Halifax Regional Municipality, Central Nova Scotia. *In* Mineral Resources Branch, Report of Activities 2007. Nova Scotia Department of Natural Resources, Report 2008-1, pp. 125–139.

White, C.E., Palacios, T., Jensen, S., and Barr, S.M. 2012. Cambrian-Ordovician acritarchs in the Meguma terrane, Nova Scotia, Canada: Resolution of early Paleozoic stratigraphy and implications for paleogeography. Geological Society of America Bulletin 124, pp. 1773–1792. http://dx.doi.org/10.1130/B30638.1

Woodman, J.E. 1904. Nomenclature of the gold-bearing metamorphic series of Nova Scotia. American Geologist, 33, pp. 363–370.

Editorial responsibility: Sandra M. Barr

Appendix A: U-Pb isotopic data for sample NB027A (Lumsden Dam Formation).

				Isotopic ratios								Apparent age (Ma) summary						
zircon	spot size	^{206}Pb (cps)	^{204}Pb (cps)	^{207}Pb/ ^{206}Pb	2σ	^{207}Pb/ ^{235}U	2σ	^{206}Pb/ ^{238}U	2σ	ρ	common Pb corrected?	^{207}Pb*/^{2} ^{06}Pb*	2σ	^{207}Pb*/ ^{235}U	2σ	^{206}Pb*/ ^{238}U	2σ	discordance %
Better than ± 10% discordant																		
NB027-007	30µ	841177	324	0.06006	0.00112	0.85807	0.04726	0.10362	0.00537	0.941	yes	606	40	629	26	636	31	-5.2
NB027-008	30µ	106014	98	0.06131	0.00110	0.84108	0.04688	0.09949	0.00525	0.946	no	650	38	620	26	611	31	6.3
NB027-011	30µ	852294	153	0.13032	0.00132	7.28714	0.46961	0.40554	0.02581	0.988	no	2102	18	2147	56	2195	117	-5.2
NB027-014	30µ	94060	168	0.06369	0.00173	0.97392	0.05402	0.11090	0.00537	0.872	no	731	56	690	27	678	31	7.7
NB027-015	30µ	244625	151	0.07667	0.00098	1.86015	0.09415	0.17596	0.00862	0.968	no	1113	25	1067	33	1045	47	6.6
NB027-016	30µ	357464	111	0.06105	0.00076	0.88507	0.04218	0.10515	0.00484	0.966	no	641	26	644	22	645	28	-0.6
NB027-019	30µ	1401723	263	0.12287	0.00144	5.73042	0.28815	0.33824	0.01654	0.972	yes	1998	21	1936	43	1878	79	6.9
NB027-022	30µ	364456	166	0.06059	0.00070	0.82893	0.05035	0.09923	0.00592	0.982	no	625	25	613	28	610	35	2.5
NB027-028	30µ	718193	252	0.11669	0.00163	5.35978	0.35314	0.33313	0.02145	0.977	yes	1906	25	1878	55	1854	103	3.2
NB027-031	30µ	941517	776	0.06185	0.00135	0.85454	0.06125	0.10020	0.00684	0.952	yes	669	46	627	33	616	40	8.4
NB027-032	30µ	458382	153	0.06900	0.00106	1.29923	0.06806	0.13657	0.00684	0.956	no	899	31	845	30	825	39	8.7
NB027-033	30µ	265131	138	0.13099	0.00192	6.67003	0.38300	0.36931	0.02050	0.967	no	2111	26	2069	49	2026	96	4.7
NB027-034	30µ	378954	167	0.06215	0.00159	0.86416	0.07244	0.10085	0.00805	0.952	no	679	54	632	39	619	47	9.2
NB027-035	30µ	218831	105	0.06341	0.00211	0.98464	0.12345	0.11261	0.01361	0.964	no	722	69	696	61	688	78	5.0
NB027-036	30µ	788664	159	0.06017	0.00106	0.82514	0.06678	0.09945	0.00786	0.976	no	610	38	611	36	611	46	-0.2
NB027-041B	20µ	758693	283	0.06497	0.00130	1.08089	0.10579	0.12066	0.01156	0.979	yes	773	41	744	50	734	66	5.3
NB027-042	30µ	811513	817	0.06086	0.00157	0.86495	0.05530	0.10308	0.00603	0.915	yes	634	54	633	30	632	35	0.3
NB027-044	30µ	648152	958	0.06085	0.00223	0.83588	0.05740	0.09962	0.00579	0.846	yes	634	77	617	31	612	34	3.6
NB027-045	30µ	378919	55	0.12635	0.00134	6.35829	0.38292	0.36498	0.02164	0.984	no	2048	19	2027	52	2006	101	2.4
NB027-047	30µ	964118	546	0.07131	0.00131	1.67815	0.08621	0.17067	0.00819	0.934	yes	966	37	1000	32	1016	45	-5.5
NB027-051	30µ	644226	1019	0.06127	0.00221	0.87469	0.06133	0.10355	0.00622	0.857	yes	649	76	638	33	635	36	2.2
NB027-053	30µ	861315	82	0.12881	0.00136	7.01007	0.53295	0.39470	0.02972	0.990	no	2082	19	2113	65	2145	136	-3.5
NB027-054	30µ	1313991	89	0.15534	0.00160	9.36136	0.49697	0.43707	0.02276	0.981	no	2406	17	2374	48	2338	101	3.4
NB027-055	30µ	619325	202	0.06093	0.00158	0.78206	0.06713	0.09309	0.00762	0.953	no	637	55	587	38	574	45	10.4
NB027-057	30µ	1320690	762	0.12167	0.00161	6.29548	0.34768	0.37527	0.02012	0.971	yes	1981	23	2018	47	2054	94	-4.3
NB027-059	30µ	420796	716	0.06188	0.00276	0.97215	0.06812	0.11394	0.00616	0.771	yes	670	93	690	34	696	36	-4.0
NB027-061	30µ	743026	181	0.06291	0.00081	0.98194	0.05666	0.11320	0.00637	0.975	no	705	27	695	29	691	37	2.1
NB027-062	30µ	465102	1031	0.06014	0.00317	0.85196	0.06145	0.10274	0.00505	0.682	yes	609	110	626	33	630	29	-3.7
NB027-073	30µ	718034	69	0.19729	0.00250	14.69977	2.02166	0.54038	0.07400	0.996	no	2804	21	2796	123	2785	302	0.8
NB027-078	30µ	293873	434	0.06966	0.00290	1.48134	0.10596	0.15424	0.00897	0.813	yes	918	83	923	42	925	50	-0.7

Appendix A. Continued.

		Isotopic ratios										Apparent age (Ma) summary						
zircon	spot size	^{206}Pb (cps)	^{204}Pb (cps)	^{207}Pb/ ^{206}Pb	2σ	^{207}Pb/ ^{235}U	2σ	^{206}Pb/ ^{238}U	2σ	ρ	common Pb corrected?	^{207}Pb*/^{2} ^{06}Pb*	2σ	^{207}Pb*/ ^{235}U	2σ	^{206}Pb*/ ^{238}U	2σ	discordance %
NB027-080	30µ	716699	84	0.17543	0.00198	11.38427	0.79035	0.47066	0.03224	0.987	no	2610	19	2555	63	2486	140	5.7
NB027-081	30µ	558953	49	0.12574	0.00137	6.45590	0.34615	0.37237	0.01955	0.979	no	2039	19	2040	46	2041	91	-0.1
NB027-089	30µ	195258	818	0.05871	0.00630	0.72037	0.08906	0.08899	0.00545	0.496	yes	556	218	551	51	550	32	1.3
NB027-090	30µ	631245	3	0.11649	0.00133	5.09256	0.31716	0.31706	0.01941	0.983	no	1903	20	1835	52	1775	94	7.7
NB027-109	30µ	133944	31	0.06242	0.00108	0.95721	0.03946	0.11122	0.00417	0.908	no	689	36	682	20	680	24	1.3
NB027-111	30µ	1014140	4361	0.06198	0.00462	0.85541	0.10515	0.10010	0.00978	0.795	yes	673	152	628	56	615	57	9.1
NB027-124	30µ	139967	34	0.06086	0.00123	0.81468	0.06021	0.09708	0.00690	0.962	no	634	43	605	33	597	40	6.1
NB027-130	30µ	159698	100	0.13289	0.00274	6.37948	0.57342	0.34818	0.03046	0.973	no	2136	36	2029	76	1926	144	11.4
NB027-133	30µ	366355	30	0.05982	0.00071	0.75743	0.04012	0.09184	0.00474	0.975	no	597	25	573	23	566	28	5.4
NB027-134	30µ	103084	31	0.09019	0.00145	2.95722	0.22118	0.23781	0.01737	0.977	no	1430	30	1397	55	1375	90	4.2
NB027-140	30µ	297381	12	0.06124	0.00078	0.83121	0.05096	0.09844	0.00590	0.978	no	648	27	614	28	605	35	6.9
NB027-150	30µ	775281	695	0.06295	0.00158	0.96793	0.08618	0.11153	0.00953	0.959	yes	706	53	687	44	682	55	3.7
Discordance >10% or <-10%																		
NB027-001	30µ	312011	500	0.06831	0.00329	0.87007	0.06847	0.09238	0.00575	0.791	no	878	97	636	37	570	34	36.7
NB027-002	30µ	761848	840	0.05474	0.00160	0.78838	0.05564	0.10446	0.00671	0.911	yes	401	64	590	31	641	39	-62.6
NB027-003	30µ	82722	294	0.06470	0.00291	0.79823	0.07135	0.08948	0.00691	0.864	no	765	92	596	40	552	41	28.9
NB027-004	30µ	1771085	507	0.13546	0.00157	5.23192	0.33379	0.28012	0.01758	0.983	yes	2170	20	1858	53	1592	88	30.0
NB027-005	30µ	508295	530	0.05068	0.00189	0.65456	0.05687	0.09368	0.00735	0.903	yes	226	84	511	34	577	43	-162.3
NB027-006	30µ	49127	100	0.06554	0.00179	0.98968	0.05779	0.10952	0.00565	0.884	no	792	56	699	29	670	33	16.2
NB027-009	30µ	397851	205	0.06306	0.00146	0.88805	0.05062	0.10214	0.00532	0.914	no	710	48	645	27	627	31	12.3
NB027-010	30µ	259853	140	0.07404	0.00151	1.45720	0.10622	0.14274	0.00999	0.960	no	1043	41	913	43	860	56	18.7
NB027-012	30µ	21088	125	0.07377	0.00456	1.56856	0.19525	0.15422	0.01666	0.868	no	1035	120	958	74	925	92	11.5
NB027-013	30µ	474233	195	0.11038	0.00120	3.60233	0.25397	0.23670	0.01649	0.988	no	1806	20	1550	55	1369	85	26.8
NB027-017	30µ	124463	148	0.06202	0.00087	0.82459	0.05308	0.09643	0.00606	0.976	no	675	30	611	29	593	36	12.6
NB027-018	30µ	688774	137	0.13058	0.00150	5.74465	0.43969	0.31906	0.02414	0.989	no	2106	20	1938	64	1785	117	17.4
NB027-020	30µ	651631	215	0.12453	0.00176	4.20614	0.30395	0.24497	0.01736	0.981	no	2022	25	1675	58	1413	89	33.5
NB027-021	30µ	64510	159	0.06451	0.00202	0.95013	0.04906	0.10682	0.00438	0.795	no	758	65	678	25	654	25	14.4
NB027-023B	20µ	1071	29	0.16485	0.24486	0.69856	4.60668	0.03073	0.19746	0.974	no	2506	1439	538	1332	195	1130	93.5
NB027-024	30µ	207168	240	0.06293	0.00131	0.86788	0.05076	0.10002	0.00547	0.935	no	706	44	634	27	615	32	13.6
NB027-025	30µ	608298	368	0.15803	0.00175	8.75937	0.75325	0.40200	0.03428	0.992	no	2435	19	2313	75	2178	156	12.4

Appendix A. Continued.

		Isotopic ratios										Apparent age (Ma) summary						
zircon	spot size	^{206}Pb (cps)	^{204}Pb (cps)	^{207}Pb/ ^{206}Pb	2σ	^{207}Pb/ ^{235}U	2σ	^{206}Pb/ ^{238}U	2σ	ρ	common Pb corrected?	^{207}Pb*/^{2} ^{06}Pb*	2σ	^{207}Pb*/ ^{235}U	2σ	^{206}Pb*/ ^{238}U	2σ	discordance %
NB027-026	30µ	230836	1756	0.04679	0.00977	0.55826	0.12449	0.08652	0.00679	0.352	yes	39	436	450	78	535	40	-1334.2
NB027-027	30µ	136656	303	0.03002	0.00620	0.37898	0.08275	0.09155	0.00646	0.323	yes	-1157	543	326	59	565	38	155.7
NB027-029	30µ	412214	282	0.05273	0.00210	0.72753	0.07227	0.10007	0.00911	0.916	yes	317	88	555	42	615	53	-98.5
NB027-030	30µ	254299	348	0.05555	0.00285	0.88149	0.07293	0.11508	0.00747	0.784	yes	435	110	642	39	702	43	-65.0
NB027-037	30µ	111273	194	0.08146	0.00388	1.14999	0.08617	0.10239	0.00592	0.771	no	1233	91	777	40	628	35	51.4
NB027-038	30µ	252555	653	0.10891	0.00402	4.21883	0.56295	0.28093	0.03603	0.961	yes	1781	66	1678	104	1596	179	11.7
NB027-039	30µ	455433	1517	0.05831	0.00400	0.87092	0.09969	0.10833	0.00992	0.800	yes	541	143	636	53	663	57	-23.7
NB027-040	30µ	396952	626	0.17916	0.00477	10.47609	0.69732	0.42408	0.02588	0.917	yes	2645	43	2478	60	2279	116	16.4
NB027-043	30µ	498484	284	0.11140	0.00191	3.68316	0.23332	0.23978	0.01462	0.963	yes	1822	31	1568	49	1386	76	26.6
NB027-046	30µ	67083	133	0.09241	0.00547	1.50976	0.15919	0.11849	0.01034	0.827	no	1476	108	934	62	722	59	53.9
NB027-048	30µ	135128	218	0.08153	0.00261	1.22122	0.09065	0.10864	0.00728	0.902	no	1234	61	810	41	665	42	48.5
NB027-049	30µ	131372	678	0.05315	0.00918	0.68839	0.12421	0.09393	0.00492	0.290	yes	335	350	532	72	579	29	-75.9
NB027-050	30µ	470173	162	0.15265	0.00164	7.23579	0.30256	0.34378	0.01389	0.967	no	2376	18	2141	37	1905	66	22.9
NB027-052	30µ	57793	241	0.09759	0.01642	1.45534	0.26618	0.10816	0.00775	0.392	no	1578	286	912	105	662	45	61.0
NB027-056	20µ	1450830	1261	0.08977	0.00140	1.84055	0.13356	0.14871	0.01054	0.977	yes	1421	30	1060	47	894	59	39.7
NB027-058	20µ	550078	1865	0.07309	0.00417	1.15337	0.10519	0.11445	0.00814	0.780	yes	1016	112	779	48	699	47	33.0
NB027-060	30µ	488718	219	0.06938	0.00089	1.12944	0.05924	0.11807	0.00601	0.970	no	910	26	767	28	719	35	22.1
NB027-063	30µ	350	28	0.82066	0.37679	7.99886	10.39351	0.07069	0.08593	0.935	no	4958	531	2231	780	440	498	93.9
NB027-064	30µ	625519	2313	0.10830	0.00419	5.42479	0.54570	0.36330	0.03373	0.923	yes	1771	69	1889	83	1998	158	-14.9
NB027-066	30µ	7684	179	0.27164	0.08561	4.74566	1.95414	0.12671	0.03358	0.644	no	3316	423	1775	297	769	189	81.2
NB027-067	30µ	3728	116	0.72530	0.05755	34.33444	89.81677	0.34333	0.89771	1.000	no	4782	109	3620	1284	1903	3299	68.8
NB027-068	30µ	1555	59	0.84058	0.14341	16.45190	12.44400	0.14195	0.10460	0.974	no	4992	223	2903	547	856	565	87.9
NB027-069	30µ	2377	88	0.64644	0.06339	23.76819	16.63303	0.26666	0.18477	0.990	no	4616	135	3259	522	1524	878	74.5
NB027-070	30µ	9809	81	0.21541	0.03174	5.11889	1.32248	0.17235	0.03657	0.821	no	2947	220	1839	199	1025	198	70.3
NB027-071	30µ	952446	7304	0.06218	0.00854	0.83303	0.14023	0.09716	0.00946	0.578	yes	680	269	615	75	598	55	12.7
NB027-072	30µ	319457	108	0.06814	0.00618	0.96249	0.20591	0.10244	0.01985	0.906	no	873	177	685	101	629	115	29.4
NB027-074	30µ	404279	1671	0.08703	0.00542	1.55169	0.14142	0.12931	0.00861	0.730	yes	1361	115	951	55	784	49	45.0
NB027-076	30µ	214472	68	0.06239	0.00093	0.75071	0.03856	0.08727	0.00429	0.957	no	688	32	569	22	539	25	22.5
NB027-077	30µ	206076	26	0.06390	0.00151	0.94069	0.09658	0.10677	0.01067	0.973	no	738	49	673	49	654	62	12.0
NB027-079	30µ	171483	312	0.08561	0.00619	1.23347	0.10955	0.10450	0.00539	0.581	no	1329	134	816	49	641	31	54.4

Appendix A. Continued.

		Isotopic ratios										Apparent age (Ma) summary						
zircon	spot size	^{206}Pb (cps)	^{204}Pb (cps)	^{207}Pb/ ^{206}Pb	2σ	^{207}Pb/ ^{235}U	2σ	^{206}Pb/ ^{238}U	2σ	ρ	common Pb corrected?	^{207}Pb*/^{2} ^{06}Pb*	2σ	^{207}Pb*/ ^{235}U	2σ	^{206}Pb*/ ^{238}U	2σ	discordance %
NB027-082	30µ	145946	450	0.32565	0.08775	8.16625	2.95314	0.18187	0.04387	0.667	yes	3597	362	2250	284	1077	235	75.7
NB027-084	30µ	183348	475	0.10628	0.00494	3.13901	0.47687	0.21420	0.03098	0.952	yes	1737	83	1442	111	1251	162	30.7
NB027-085	30µ	115534	131	0.07322	0.00254	1.08444	0.09256	0.10742	0.00837	0.913	no	1020	69	746	44	658	49	37.3
NB027-086	30µ	210034	186	0.07374	0.00199	0.94345	0.05300	0.09279	0.00457	0.876	no	1034	54	675	27	572	27	46.7
NB027-087	30µ	5228	286	0.73926	1.85621	53.03100	170.08324	0.52027	1.03817	0.622	yes	4809	1738	4051	1444	2700	3355	53.1
NB027-088	30µ	2749	24	0.20117	0.05962	3.75597	1.65988	0.13541	0.04439	0.742	no	2836	416	1583	304	819	247	75.5
NB027-092	30µ	273887	942	0.06549	0.00467	0.81069	0.06622	0.08978	0.00358	0.489	yes	790	143	603	36	554	21	31.2
NB027-094	30µ	945	35	0.72646	0.15868	12.77865	20.22466	0.12758	0.19998	0.990	no	4784	281	2663	917	774	1053	88.4
NB027-097	30µ	338417	53	0.06345	0.00122	0.81225	0.04724	0.09285	0.00510	0.944	no	723	40	604	26	572	30	21.8
NB027-099	30µ	672720	465	0.19040	0.00256	8.68964	0.54238	0.33100	0.02018	0.977	yes	2746	22	2306	55	1843	97	37.7
NB027-100	30µ	4829	153	0.61604	0.03751	68.19780	130.66809	0.80289	1.53758	0.999	no	4546	86	4302	1077	3799	3976	21.6
NB027-101	30µ	2004	163	0.84362	0.10954	10.63275	22.67614	0.09141	0.19459	0.998	no	4997	173	2492	1098	564	1058	92.2
NB027-102	30µ	271077	158	0.07112	0.00151	1.02560	0.06266	0.10458	0.00599	0.937	no	961	43	717	31	641	35	34.9
NB027-103	30µ	1866	158	0.76290	0.05168	32.70190	27.08734	0.31089	0.25665	0.997	no	4854	93	3572	599	1745	1153	72.3
NB027-104	30µ	252304	180	0.06570	0.00175	0.89408	0.06169	0.09869	0.00628	0.923	no	797	55	649	33	607	37	25.0
NB027-105	30µ	168217	130	0.06756	0.00169	0.87108	0.07198	0.09351	0.00736	0.953	no	855	51	636	38	576	43	34.1
NB027-106	30µ	1109753	345	0.09745	0.00229	2.24170	0.19923	0.16683	0.01430	0.964	yes	1576	43	1194	61	995	79	39.8
NB027-107	30µ	1506	55	0.54311	0.14347	8.85451	21.47358	0.11824	0.28505	0.994	no	4363	340	2323	1174	720	1464	87.8
NB027-108	30µ	624701	211	0.06942	0.00154	1.15456	0.08376	0.12062	0.00833	0.952	no	911	45	779	39	734	48	20.6
NB027-110	30µ	624029	192	0.12180	0.00209	3.88030	0.35574	0.23105	0.02081	0.982	no	1983	30	1610	71	1340	108	35.8
NB027-113	30µ	475	14	0.40554	0.59372	7.16694	24.84586	0.12817	0.40278	0.906	no	3930	1307	2132	1418	777	1968	84.7
NB027-114	30µ	474793	208	0.11580	0.00147	4.22928	0.34021	0.26489	0.02104	0.987	no	1892	23	1680	64	1515	106	22.4
NB027-115	30µ	804396	241	0.06465	0.00097	0.91606	0.05114	0.10277	0.00553	0.963	no	763	31	660	27	631	32	18.2
NB027-116	30µ	462354	6984	0.06935	0.01753	0.92616	0.24262	0.09686	0.00666	0.263	yes	909	449	666	120	596	39	36.0
NB027-117	30µ	2006	62	0.70449	0.10990	52.34171	42.40464	0.53886	0.42839	0.981	no	4740	207	4038	594	2779	1583	50.4
NB027-118	30µ	154442	543	0.06486	0.00562	0.78303	0.14138	0.08756	0.01387	0.877	yes	770	172	587	77	541	82	31.0
NB027-119	30µ	6104	155	0.44072	0.06364	15.22470	6.42413	0.25054	0.09933	0.940	no	4054	200	2829	339	1441	493	71.4
NB027-120	30µ	251761	556	0.06210	0.00700	0.65680	0.09905	0.07671	0.00769	0.664	yes	678	224	513	59	476	46	30.8
NB027-121	30µ	41019	198	0.10678	0.01165	1.65331	0.21727	0.11230	0.00823	0.558	no	1745	187	991	80	686	48	63.9
NB027-122	30µ	217380	172	0.06902	0.00246	0.93745	0.07603	0.09851	0.00718	0.898	no	899	72	672	39	606	42	34.2

		Isotopic ratios										Apparent age (Ma) summary					
zircon	spot size	^{206}Pb (cps)	^{204}Pb (cps)	^{207}Pb/ ^{206}Pb	2σ	^{207}Pb/ ^{235}U	2σ	^{206}Pb/ ^{238}U	2σ	ρ	common Pb corrected?	^{207}Pb*/^{2} ^{06}Pb*	2σ	^{207}Pb*/ ^{235}U	2σ	^{206}Pb*/ ^{238}U	2σ
NB027-123	30µ	73937	51	0.06527	0.00220	0.89839	0.07424	0.09983	0.00753	0.913	no	783	69	651	39	613	44
NB027-127	30µ	829305	1438	0.08222	0.00218	1.86608	0.16282	0.16461	0.01368	0.953	yes	1251	51	1069	56	982	75
NB027-129	30µ	9928	76	0.25615	0.15638	11.82168	15.73807	0.33473	0.39600	0.889	no	3223	732	2590	813	1861	1675
NB027-131	30µ	253791	78	0.06399	0.00123	0.89870	0.04498	0.10186	0.00470	0.923	no	741	40	651	24	625	27
NB027-135	30µ	81051	111	0.07187	0.00307	0.97949	0.09571	0.09884	0.00869	0.900	no	982	85	693	48	608	51
NB027-136	30µ	398732	106	0.09455	0.00244	2.02005	0.21041	0.15496	0.01564	0.969	no	1519	48	1122	68	929	87
NB027-137	30µ	1010069	460	0.18429	0.00419	8.53414	0.67778	0.33585	0.02555	0.958	yes	2692	37	2290	70	1867	122
NB027-138	30µ	17675	52	0.08665	0.00811	1.42140	0.17871	0.11898	0.00999	0.668	no	1353	171	898	72	725	57
NB027-139	30µ	1211	51	0.96505	0.59566	23.43784	59.14662	0.17614	0.43101	0.970	no	5187	668	3245	1249	1046	2013
NB027-142	30µ	54340	9	0.06309	0.00178	0.90043	0.05184	0.10351	0.00519	0.871	no	711	59	652	27	635	30
NB027-143	30µ	23874	35	0.07818	0.00970	1.14812	0.17703	0.10651	0.00975	0.594	no	1152	228	776	80	652	57
NB027-144	30µ	388112	1170	0.06565	0.00372	0.77239	0.08491	0.08534	0.00804	0.857	yes	795	114	581	48	528	48
NB027-145	30µ	8136	1	0.07040	0.01161	1.10457	0.20138	0.11379	0.00885	0.427	no	940	306	756	93	695	51
NB027-146	30µ	81009	35	0.06623	0.00300	0.91464	0.08097	0.10016	0.00762	0.859	no	814	92	660	42	615	44
NB027-148	30µ	120637	93	0.08338	0.00804	1.12442	0.15238	0.09781	0.00932	0.703	no	1278	177	765	70	602	54

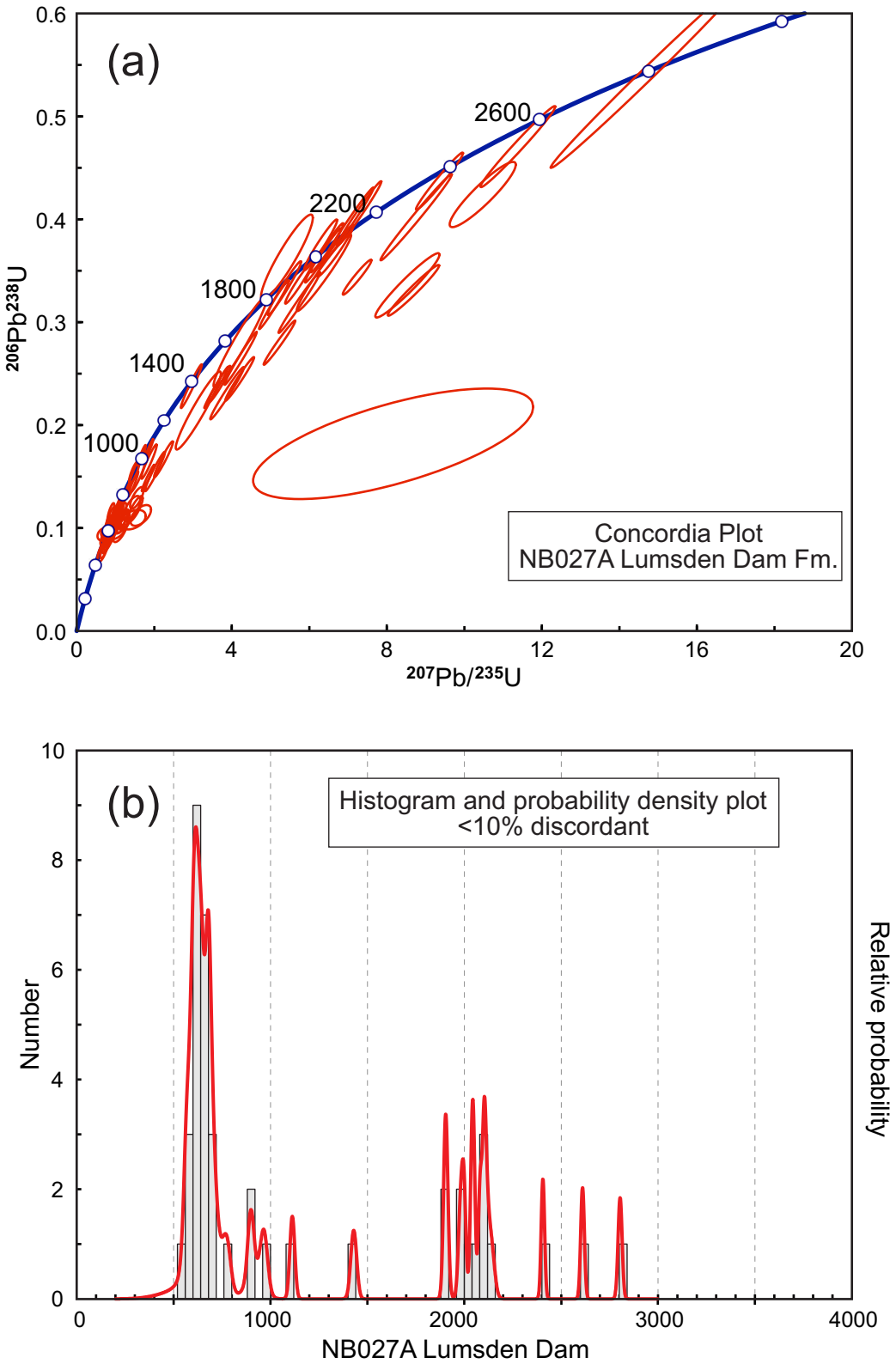

Figure A. U-Pb data for detrital zircons from the Lumsden Dam Formation. (a) U-Pb concordia plot. Errors are shown at the two sigma level. (b) Probability density curve and histograms of detrital zircon. Data shown are for U–Pb analyses that are <10% discordant: $^{207}Pb/^{206}Pb$ ages for analyses >800 Ma, and $^{206}Pb/^{238}U$ ages are analyses <800 Ma.

Appendix B: U-Pb isotopic data for sample LR080B (Glen Brook Formation).

				Isotopic ratios								Apparent age (Ma) summary						
zircon	spot size	^{206}Pb (cps)	^{204}Pb (cps)	^{207}Pb/ ^{206}Pb	2σ	^{207}Pb/ ^{235}U	2σ	^{206}Pb/ ^{238}U	2σ	ρ	common Pb corrected?	^{207}Pb*/^{2} ^{06}Pb*	2σ	^{207}Pb*/ ^{235}U	2σ	^{206}Pb*/ ^{238}U	2σ	discordance %
Better than ± 10% discordant																		
LR080B-1	30µ	34896	33	0.06218	0.00119	0.90956	0.03964	0.10609	0.00415	0.898	no	680	40	657	21	650	24	4.7
LR080B-3	30µ	78836	57	0.06117	0.00076	0.85680	0.04469	0.10160	0.00515	0.972	no	645	26	628	24	624	30	3.5
LR080B-6	30µ	68088	57	0.06146	0.00076	0.94908	0.03809	0.11199	0.00427	0.951	no	655	26	678	20	684	25	-4.6
LR080B-7	30µ	211842	86	0.06090	0.00069	0.87455	0.03779	0.10416	0.00434	0.965	no	636	24	638	20	639	25	-0.5
LR080B-11	30µ	310909	165	0.06155	0.00126	0.82688	0.03473	0.09743	0.00357	0.873	no	659	43	612	19	599	21	9.4
LR080B-12	30µ	212146	83	0.12810	0.00142	6.57349	0.25346	0.37217	0.01375	0.958	no	2072	19	2056	33	2040	64	1.8
LR080B-13	30µ	383500	85	0.12766	0.00149	6.33515	0.26221	0.35992	0.01429	0.960	no	2066	20	2023	36	1982	67	4.7
LR080B-14	30µ	34014	74	0.05969	0.00083	0.78457	0.03134	0.09533	0.00357	0.937	no	592	30	588	18	587	21	0.9
LR080B-15	30µ	244992	50	0.06157	0.00104	0.92651	0.03773	0.10913	0.00404	0.910	no	659	36	666	20	668	23	-1.3
LR080B-20	30µ	369889	70	0.12365	0.00131	6.03886	0.23466	0.35420	0.01324	0.962	no	2010	19	1981	33	1955	63	3.2
LR080B-21	30µ	127220	90	0.06354	0.00087	0.95005	0.03699	0.10844	0.00395	0.936	no	726	29	678	19	664	23	9.1
LR080B-30	30µ	1060335	204	0.14592	0.00176	8.53524	0.35182	0.42422	0.01673	0.956	no	2299	21	2290	37	2280	75	1.0
LR080B-32	30µ	178570	94	0.11704	0.00308	5.07941	0.24065	0.31475	0.01240	0.832	no	1912	46	1833	39	1764	61	8.8
LR080B-33	30µ	440401	31	0.12416	0.00137	5.85362	0.22049	0.34193	0.01232	0.956	no	2017	19	1954	32	1896	59	6.9
LR080B-39	30µ	558536	320	0.13377	0.00154	6.72314	0.30082	0.36451	0.01576	0.966	no	2148	20	2076	39	2004	74	7.8
LR080B-40	20µ	306099	152	0.12404	0.00132	6.18249	0.24950	0.36150	0.01407	0.964	no	2015	19	2002	35	1989	66	1.5
LR080B-41	30µ	11757	101	0.06157	0.00129	0.91231	0.04508	0.10747	0.00481	0.906	no	659	44	658	24	658	28	0.2
LR080B-44	30µ	161140	140	0.13015	0.00136	6.80951	0.28404	0.37945	0.01533	0.968	no	2100	18	2087	36	2074	71	1.5
LR080B-46	30µ	160372	74	0.12540	0.00214	5.89811	0.27327	0.34112	0.01469	0.930	no	2034	30	1961	39	1892	70	8.1
LR080B-48	30µ	653390	200	0.12463	0.00197	6.39804	0.28818	0.37233	0.01571	0.937	no	2024	28	2032	39	2040	73	-1.0
LR080B-50	30µ	2431200	2608	0.20464	0.00226	14.58317	0.63886	0.51685	0.02191	0.968	no	2864	18	2788	41	2686	92	7.6
LR080B-51	30µ	1333309	630	0.13624	0.00149	7.02258	0.26739	0.37386	0.01364	0.958	no	2180	19	2114	33	2048	64	7.1
LR080B-55	30µ	2871625	1346	0.19390	0.00197	15.50960	0.72854	0.58012	0.02661	0.976	no	2776	17	2847	44	2949	108	-7.8
LR080B-56	30µ	229573	1112	0.12554	0.00130	6.52092	0.33400	0.37671	0.01889	0.979	no	2036	18	2049	44	2061	88	-1.4
LR080B-58	30µ	791800	1043	0.13811	0.00216	7.42204	0.36398	0.38977	0.01811	0.948	no	2204	27	2164	43	2122	83	4.4
LR080B-61	30µ	251383	796	0.06045	0.00091	0.83654	0.03865	0.10037	0.00439	0.946	no	620	32	617	21	617	26	0.5
LR080B-62	30µ	81817	423	0.06090	0.00079	0.89100	0.03924	0.10612	0.00447	0.955	no	636	28	647	21	650	26	-2.4
LR080B-63	30µ	227767	1063	0.06375	0.00169	0.96699	0.04932	0.11001	0.00479	0.854	no	733	55	687	25	673	28	8.7
LR080B-64	30µ	136484	318	0.12831	0.00160	6.23059	0.30273	0.35218	0.01654	0.967	no	2075	22	2009	42	1945	78	7.3
LR080B-67	30µ	39129	858	0.06306	0.00123	0.96690	0.05151	0.11121	0.00551	0.930	no	710	41	687	26	680	32	4.5

Appendix B. Continued.

				Isotopic ratios								Apparent age (Ma) summary						
zircon	spot size	^{206}Pb (cps)	^{204}Pb (cps)	^{207}Pb/ ^{206}Pb	2σ	^{207}Pb/ ^{235}U	2σ	^{206}Pb/ ^{238}U	2σ	ρ	common Pb corrected?	^{207}Pb*/^{2} ^{06}Pb*	2σ	^{207}Pb*/ ^{235}U	2σ	^{206}Pb*/ ^{238}U	2σ	discordance %
LR080B-68	30µ	441333	516	0.11821	0.00138	5.47882	0.26630	0.33615	0.01586	0.971	no	1929	21	1897	41	1868	76	3.7
LR080B-75	30µ	2026485	2460	0.16330	0.00244	10.10867	0.43756	0.44895	0.01824	0.938	no	2490	25	2445	39	2391	81	4.8
LR080B-76	30µ	1016753	1044	0.12368	0.00128	6.22226	0.25836	0.36487	0.01467	0.969	no	2010	18	2008	36	2005	69	0.3
LR080B-77	30µ	1579553	1924	0.18031	0.00307	11.99929	0.68265	0.48266	0.02620	0.954	no	2656	28	2604	52	2539	113	5.3
LR080B-78	30µ	1953538	1419	0.13609	0.00167	7.59276	0.31810	0.40464	0.01621	0.956	no	2178	21	2184	37	2190	74	-0.7
LR080B-79	30µ	976548	902	0.11157	0.00115	5.36406	0.25896	0.34870	0.01645	0.977	no	1825	19	1879	40	1928	78	-6.5
LR080B-81	30µ	231332	916	0.10735	0.00116	4.65945	0.25785	0.31481	0.01708	0.981	no	1755	20	1760	45	1764	83	-0.6
LR080B-82	30µ	136953	985	0.06225	0.00155	0.91304	0.04541	0.10639	0.00458	0.865	no	683	52	659	24	652	27	4.7
LR080B-83	30µ	346825	334	0.11809	0.00124	5.09742	0.29505	0.31306	0.01782	0.983	no	1928	19	1836	48	1756	87	10.2
LR080B-86	30µ	420230	687	0.05820	0.00103	0.66312	0.03637	0.08263	0.00429	0.947	no	537	38	517	22	512	25	5.0
LR080B-90	30µ	1636682	4096	0.15283	0.00348	8.43424	0.86827	0.40026	0.04018	0.975	no	2378	38	2279	89	2170	182	10.3
LR080B-91	30µ	573936	1251	0.12995	0.00176	6.38618	0.37917	0.35642	0.02060	0.974	no	2097	24	2030	51	1965	97	7.3
LR080B-102	30µ	453662	900	0.18398	0.00361	12.32540	0.58129	0.48588	0.02084	0.909	no	2689	32	2630	43	2553	90	6.1
LR080B-105	30µ	1155168	679	0.14308	0.00151	7.77886	0.32159	0.39431	0.01576	0.967	no	2265	18	2206	37	2143	72	6.3
LR080B-106	30µ	320069	639	0.05946	0.00068	0.81056	0.03627	0.09886	0.00428	0.967	no	584	25	603	20	608	25	-4.2
LR080B-107	30µ	575932	1132	0.14029	0.00308	7.22822	0.40223	0.37369	0.01911	0.919	no	2231	37	2140	48	2047	89	9.6
LR080B-109	30µ	186969	11420	0.79714	0.02477	131.80235	47.04576	1.19919	0.42642	0.996	no	4917	44	4964	308	5080	1142	-4.8
Discordance >10% or <-10%																		
LR080B-2	30µ	20549	28	0.06014	0.00100	0.93917	0.03857	0.11326	0.00425	0.914	no	609	36	672	20	692	25	-14.4
LR080B-4	30µ	284458	106	0.15008	0.00170	7.28502	0.29931	0.35204	0.01391	0.961	no	2347	19	2147	36	1944	66	19.8
LR080B-5	30µ	205454	184	0.10567	0.00331	3.23100	0.20810	0.22176	0.01248	0.874	no	1726	56	1465	49	1291	66	27.8
LR080B-8	30µ	140576	573	0.10849	0.00686	1.53930	0.11232	0.10290	0.00374	0.499	no	1774	111	946	44	631	22	67.5
LR080B-9	30µ	262019	560	0.09047	0.00583	1.37238	0.10137	0.11002	0.00397	0.488	no	1435	118	877	42	673	23	55.9
LR080B-10	30µ	115578	96	0.09579	0.00345	2.52829	0.22356	0.19142	0.01546	0.913	no	1544	66	1280	62	1129	83	29.3
LR080B-16	30µ	176452	615	0.10226	0.00835	1.44620	0.13308	0.10257	0.00435	0.461	no	1666	144	908	54	629	25	65.2
LR080B-17	30µ	221072	1410	0.13983	0.01083	2.20651	0.19534	0.11445	0.00490	0.484	no	2225	128	1183	60	699	28	72.2
LR080B-18	30µ	93261	164	0.06389	0.00154	0.93830	0.03955	0.10651	0.00369	0.821	no	738	50	672	21	652	21	12.2
LR080B-19	30µ	289290	345	0.07420	0.00097	1.34360	0.05885	0.13132	0.00549	0.954	no	1047	26	865	25	795	31	25.5
LR080B-22	30µ	584760	935	0.15146	0.00443	5.26924	0.30772	0.25233	0.01276	0.866	no	2362	49	1864	49	1450	65	43.0
LR080B-23	30µ	440521	2912	0.19020	0.00610	8.62202	0.56261	0.32877	0.01868	0.871	no	2744	52	2299	58	1832	90	38.0

Appendix B. Continued.

		Isotopic ratios										Apparent age (Ma) summary						
zircon	spot size	^{206}Pb (cps)	^{204}Pb (cps)	^{207}Pb/ ^{206}Pb	2σ	^{207}Pb/ ^{235}U	2σ	^{206}Pb/ ^{238}U	2σ	ρ	common Pb corrected?	^{207}Pb*/^{2} ^{06}Pb*	2σ	^{207}Pb*/ ^{235}U	2σ	^{206}Pb*/ ^{238}U	2σ	discordance %
LR080B-24	30µ	183576	266	0.08361	0.00136	1.53140	0.08591	0.13284	0.00713	0.957	no	1283	31	943	34	804	40	39.7
LR080B-25	30µ	158020	215	0.06703	0.00161	0.91264	0.04412	0.09874	0.00414	0.868	no	839	49	658	23	607	24	28.9
LR080B-26	30µ	115163	220	0.06873	0.00269	0.95855	0.05295	0.10115	0.00394	0.705	no	891	79	683	27	621	23	31.7
LR080B-27	30µ	114545	610	0.11559	0.00690	1.65044	0.12266	0.10356	0.00459	0.596	no	1889	104	990	46	635	27	69.6
LR080B-28	20µ	156896	579	0.10664	0.00588	1.50644	0.10110	0.10245	0.00391	0.569	no	1743	98	933	40	629	23	67.0
LR080B-29	30µ	39257	131	0.09790	0.00625	1.42215	0.10789	0.10536	0.00431	0.539	no	1584	115	898	44	646	25	62.2
LR080B-31	30µ	121966	300	0.11458	0.00836	2.69814	0.23813	0.17078	0.00848	0.563	no	1873	126	1328	63	1016	47	49.4
LR080B-34	30µ	82350	73	0.06977	0.00131	0.95774	0.03999	0.09955	0.00371	0.893	no	922	38	682	21	612	22	35.2
LR080B-35	30µ	183212	128	0.07222	0.00104	1.47015	0.07051	0.14763	0.00675	0.954	no	992	29	918	29	888	38	11.3
LR080B-36	30µ	97459	90	0.07525	0.00133	1.48990	0.06987	0.14361	0.00624	0.926	no	1075	35	926	28	865	35	20.9
LR080B-37	30µ	31185	167	0.06481	0.00147	0.88741	0.04009	0.09931	0.00388	0.865	no	768	47	645	21	610	23	21.5
LR080B-38	30µ	1699128	775	0.11256	0.00161	3.19351	0.15129	0.20578	0.00929	0.953	no	1841	26	1456	36	1206	49	37.8
LR080B-42	30µ	236693	540	0.29094	0.00657	23.55771	1.32938	0.58726	0.03037	0.916	no	3423	35	3250	54	2978	122	16.2
LR080B-43	30µ	88980	112	0.07256	0.00119	1.49430	0.06716	0.14937	0.00625	0.931	no	1002	33	928	27	897	35	11.1
LR080B-45	30µ	333145	255	0.06475	0.00077	0.88487	0.04194	0.09912	0.00455	0.968	no	766	25	644	22	609	27	21.5
LR080B-47	30µ	101273	92	0.06700	0.00123	0.90275	0.04133	0.09773	0.00410	0.916	no	838	38	653	22	601	24	29.6
LR080B-49	30µ	776901	808	0.06778	0.00210	0.90877	0.05228	0.09725	0.00472	0.843	no	862	63	656	27	598	28	32.0
LR080B-52	30µ	715468	1674	0.13921	0.00266	5.77202	0.43573	0.30071	0.02196	0.967	no	2217	33	1942	63	1695	108	26.8
LR080B-53	30µ	34188	308	0.06942	0.00302	1.16522	0.06970	0.12174	0.00500	0.687	no	911	87	784	32	741	29	19.8
LR080B-54	30µ	29702	573	0.09868	0.00917	1.39659	0.16504	0.10265	0.00749	0.617	no	1599	164	887	68	630	44	63.5
LR080B-57	30µ	389242	1841	0.11311	0.00598	4.16677	0.50180	0.26718	0.02891	0.899	no	1850	93	1668	94	1526	145	19.6
LR080B-59	20µ	923695	1856	0.07475	0.00513	1.17355	0.11349	0.11387	0.00775	0.704	no	1062	132	788	52	695	45	36.4
LR080B-60	20µ	50565	1110	0.08087	0.00791	1.25835	0.14166	0.11286	0.00629	0.495	no	1218	181	827	62	689	36	45.7
LR080B-65	30µ	2862557	4213	0.14911	0.00271	7.08820	1.03688	0.34477	0.05004	0.992	no	2336	31	2123	122	1910	236	21.0
LR080B-66	30µ	576736	930	0.12647	0.00348	3.19629	0.15710	0.18330	0.00746	0.828	no	2049	48	1456	37	1085	41	51.0
LR080B-69	30µ	764983	5939	0.20961	0.01840	6.49194	0.64383	0.22463	0.01036	0.465	no	2903	136	2045	84	1306	54	60.5
LR080B-70	30µ	135469	739	0.08575	0.00622	1.18888	0.10049	0.10055	0.00437	0.514	no	1333	134	795	46	618	26	56.2
LR080B-71	30µ	155728	539	0.10415	0.00447	3.60075	0.22307	0.25074	0.01121	0.722	no	1699	77	1550	48	1442	58	16.9
LR080B-72	30µ	423186	1944	0.11314	0.00448	1.47176	0.08797	0.09434	0.00423	0.749	no	1850	70	919	36	581	25	71.6
LR080B-74	30µ	1783189	2735	0.07356	0.00154	0.93040	0.05303	0.09173	0.00486	0.930	no	1030	42	668	28	566	29	47.0

Appendix B. Continued.

			Isotopic ratios									Apparent age (Ma) summary						
zircon	spot size	^{206}Pb (cps)	^{204}Pb (cps)	^{207}Pb/ ^{206}Pb	2σ	^{207}Pb/ ^{235}U	2σ	^{206}Pb/ ^{238}U	2σ	ρ	common Pb corrected?	^{207}Pb*/^{206}Pb*	2σ	^{207}Pb*/ ^{235}U	2σ	^{206}Pb*/ ^{238}U	2σ	discordance %
LR080B-80	30µ	879659	1180	0.06754	0.00092	1.15035	0.05352	0.12353	0.00550	0.956	no	854	28	777	25	751	31	12.8
LR080B-84	30µ	906953	1635	0.14294	0.00241	6.70997	0.37635	0.34046	0.01821	0.954	no	2263	29	2074	48	1889	87	19.1
LR080B-85	30µ	654472	1342	0.09946	0.00263	3.21442	0.15549	0.23440	0.00950	0.838	no	1614	48	1461	37	1357	49	17.6
LR080B-87	30µ	356229	898	0.07077	0.00156	1.28968	0.06349	0.13217	0.00582	0.894	no	951	44	841	28	800	33	16.8
LR080B-88	30µ	295519	932	0.07917	0.00340	1.08730	0.07326	0.09961	0.00517	0.770	no	1176	83	747	35	612	30	50.2
LR080B-89	30µ	428241	877	0.07796	0.00144	0.97213	0.04956	0.09043	0.00430	0.932	no	1146	36	690	25	558	25	53.5
LR080B-92	30µ	183838	1060	0.06643	0.00104	1.38244	0.07399	0.15094	0.00772	0.956	no	820	32	881	31	906	43	-11.3
LR080B-93	30µ	473410	723	0.11964	0.00554	4.10000	0.29763	0.24855	0.01390	0.770	no	1951	80	1654	58	1431	71	29.7
LR080B-94	30µ	207545	724	0.07245	0.00478	0.93496	0.07265	0.09359	0.00384	0.528	no	999	129	670	37	577	23	44.2
LR080B-95	30µ	69335	632	0.06276	0.00128	0.82209	0.03660	0.09499	0.00376	0.889	no	700	43	609	20	585	22	17.2
LR080B-96	30µ	66400	732	0.11528	0.01009	1.55037	0.15960	0.09754	0.00528	0.526	no	1884	150	951	62	600	31	71.3
LR080B-97	30µ	302387	1271	0.09381	0.00408	1.29483	0.08720	0.10011	0.00515	0.763	no	1504	80	843	38	615	30	61.9
LR080B-98	30µ	427198	890	0.07148	0.00120	1.24831	0.05197	0.12666	0.00483	0.916	no	971	34	823	23	769	28	22.1
LR080B-99	30µ	491517	684	0.11750	0.00139	4.75471	0.25028	0.29350	0.01506	0.975	no	1918	21	1777	43	1659	75	15.3
LR080B-100	30µ	997730	3569	0.09537	0.00578	1.26696	0.09271	0.09635	0.00395	0.561	no	1535	110	831	41	593	23	64.2
LR080B-101	30µ	317212	5593	0.26898	0.01411	5.18422	0.38637	0.13978	0.00740	0.710	no	3300	80	1850	62	843	42	79.1
LR080B-103	30µ	336261	1700	0.10410	0.00378	1.32228	0.07439	0.09212	0.00396	0.764	no	1699	65	856	32	568	23	69.4
LR080B-104	30µ	483360	950	0.12998	0.00154	5.74044	0.28932	0.32031	0.01569	0.972	no	2098	21	1937	43	1791	76	16.7
LR080B-108	30µ	616354	1562	0.08124	0.00639	1.07552	0.09958	0.09601	0.00468	0.527	no	1227	147	741	48	591	27	54.2
LR080B-110	30µ	944372	1537	0.07617	0.00304	1.24749	0.07853	0.11878	0.00579	0.774	no	1100	78	822	35	724	33	36.1

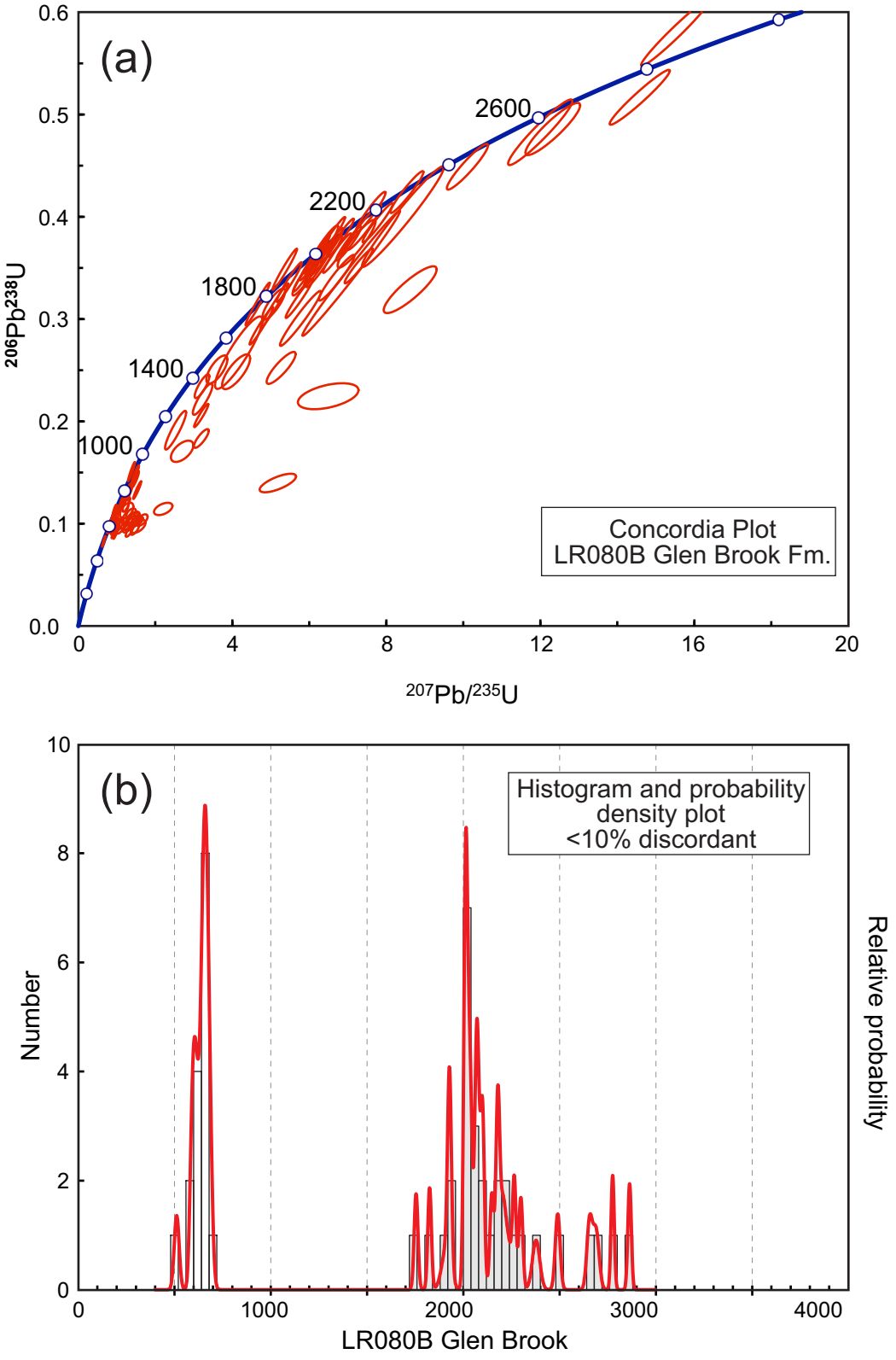

Figure B. U-Pb data for detrital zircons from the Glen Brook Formation. (a) U-Pb concordia plot. Errors are shown at the two sigma level. (b) Probability density curve and histograms of detrital zircon. Data shown are for U–Pb analyses that are <10% discordant: $^{207}Pb/^{206}Pb$ ages for analyses >800 Ma, and $^{206}Pb/^{238}U$ ages are analyses <800 Ma.